

REVIEW ARTICLE: THE USE OF REMOTELY PILOTED AIRCRAFT SYSTEMS (RPAS) FOR NATURAL HAZARDS MONITORING AND MANAGEMENT

Daniele Giordan¹, Yuichi Hayakawa², Francesco Nex³, Fabio Remondino⁴, Paolo Tarolli⁵

¹Istituto di Ricerca per la Protezione Idrogeologica, Consiglio Nazionale delle Ricerche, Italy

²Center for Spatial Information Science, The University of Tokyo, Japan

³University of Twente, Faculty of Geo-Information Science and Earth Observation (ITC), The Netherlands

⁴3D Optical Metrology (3DOM) Unit, Bruno Kessler Foundation (FBK), Trento, Italy

⁵Department of Land, Environment, Agriculture and Forestry, University of Padova, Italy

ABSTRACT

The number of scientific studies that consider possible applications of Remotely Piloted Aircraft Systems (RPAS) for the management of natural hazards effects and the identification of occurred damages are strongly increased in last decade. Nowadays, in the scientific community, the use of these systems is not a novelty, but a deeper analysis of literature shows a lack of codified complex methodologies that can be used not only for scientific experiments but also for normal codified emergency operations. RPAS can acquire on-demand ultra-high resolution images that can be used for the identification of active processes like landslides or volcanic activities but also for the definition of effects of earthquakes, wildfires and floods. In this paper, we present a review of published literature that describes experimental methodologies developed for the study and monitoring of natural hazards.

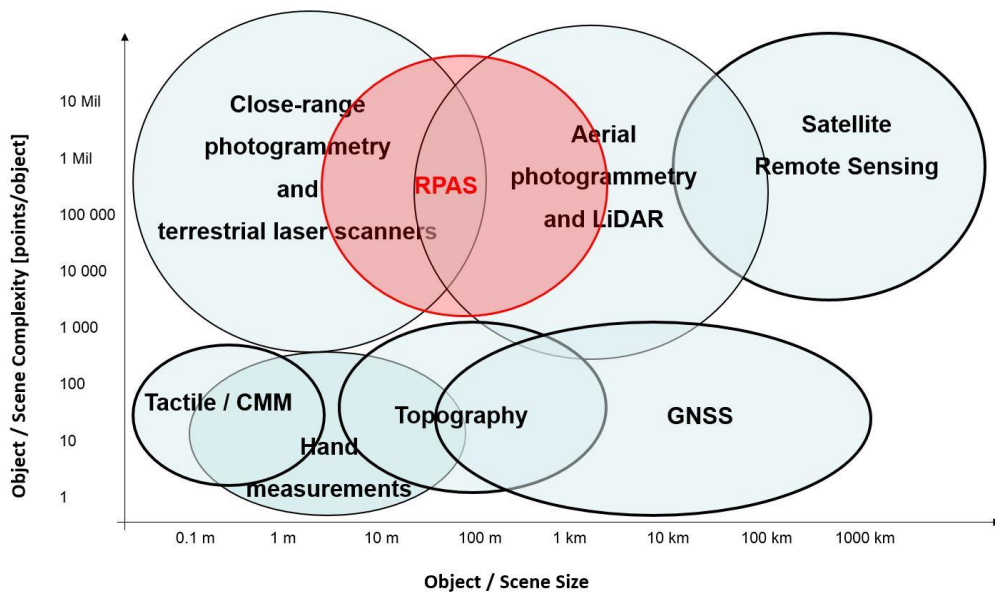
1. INTRODUCTION

In last three decades, the number of natural disasters showed a positive trend with an increase in the number of affected populations. Disasters not only affected the poor and characteristically more vulnerable countries but also those thought to be better protected. Annual Disaster Statistical Review describes recent impacts of natural disasters over population and reports 342 natural triggered disasters in 2016 (Guha-Sapir et al., 2017). This is less than the annual average disaster frequency observed from 2006 to 2015 (376.4 events), however natural disasters is still responsible for a high number of casualties (8,733 death). In the period 2006-2015, the average number of casualties annaly caused by natural disasters is 69,827. In 2016, hydrological disasters (177) had the largest share in natural disaster occurrence (51.8%), followed by meteorological disasters (96; 28.1%), climatological disasters (38; 11.1%) and geophysical disasters (31; 9.1%) (Guha-Sapir et al., 2017). To face these disasters, one of the most important solutions is the use of systems able to provide an adequate level of information for correctly understanding these events and their evolution. In this context, survey and monitoring of natural hazards gained in importance. In particular, during the emergency phase it is very important to evaluate and control the phenomenon evolution, preferably operating in near real time or real time, and consequently, use this information for a better risk scenario assessment. The available acquired data must be processed rapidly to ensure the emergency services and decision makers promptly.

39 Recently, the use of remote sensing (satellite and airborne platform) in the field of natural hazards and
40 disasters has become common, also supported by the increase in geospatial technologies and the ability to
41 provide and process up-to-date imagery (Joyce et al., 2009; Tarolli, 2014). Remotely sensed data play an
42 integral role in predicting hazard events such as floods and landslides, subsidence events and other ground
43 instabilities. Because their acquisition mode and capability for repetitive observations, the data acquired at
44 different dates and high spatial resolution can be considered as an effective complementary tool for field
45 techniques to derive information on landscape evolution and activity over wide areas.

46 In the contest of remote sensing research, recent technological developments have increased in the field of
47 Remotely Piloted Aircraft Systems (RPAS) becoming more common and widespread in civil and commercial
48 context (Bendea et al., 2008). In particular, the development of photogrammetry and technologies associated
49 (i.e. integrated camera systems like compact cameras, industrial grade cameras, video cameras, single-lens
50 reflex (SLR) digital cameras and GNSS/INS systems) allow to use of RPAS platforms in various applications as
51 alternative to the traditional remote sensing method for topographic mapping or detailed 3D recording of
52 ground information and a valid complementary solution to terrestrial acquisitions too (Nex and Remondino,
53 2014) (Fig.1).

54 RPAS systems present some advantages in comparison to traditional platforms and, in particular, they could
55 be competitive thanks to their versatility in the flight execution (Gomez and Purdie, 2016). Mini/micro RPAS
56 are the most diffused for civil purposes, and they can fly at low altitudes according to limitations defined by
57 national aviation security agencies and be easy transported into the disaster area. Foldable Systems fits easily
58 into a daypack and can be transported safely as hand luggage. This advantage is particularly important for
59 first responder teams like UNDAC or similar. Stöcker et al. (2017) published a review of different state
60 regulations that are characterized by several differences regarding requirements, distance from the takeoff
61 and maximum altitude. Another important added value of RPAS is their adaptability that allows their use in
62 various typologies of missions, and in particular for monitoring operations in remote and dangerous areas
63 (Obanawa et al., 2014). The possibility to carry out flight operations at lower costs compared to ones required
64 by traditional aircraft is also a fundamental advantage. Limited operating costs make these systems also
65 convenient for multi-temporal applications where it is often necessary to acquire information on an active
66 process (like a landslide) over the time. A comparison between the use of satellite images, traditional aircraft
67 and RPAS has been presented and discussed by Fiorucci et al. (2018) for landslides applications and by
68 Giordan et al., (2017) for the identification of flooded areas. These comparisons show that RPAS are a good
69 solution for the on demand acquisition of high resolution images over limited areas.



70

71 Figure 1. Available geomatics techniques, sensors, and platforms for topographic mapping or detailed 3D
 72 recording of ground information, according to the scene dimensions and complexity (modified from Nex and
 73 Remondino, 2014).

74 RPASs are used in several fields as agriculture, forestry, archaeology and architecture, traffic monitoring,
 75 environment and emergency management. In particular, in the field of emergency assistance and
 76 management, RPAS platforms are used to reliably and fast collect data of inaccessible areas. Collected data
 77 can be mostly images but also gas concentrations or radioactivity levels as demonstrated by the tragic event
 78 in Fukushima (Sanada and Torii, 2015; Martin et al., 2016). Focusing on image collection, they can be used
 79 for early impact assessment, to inspect collapsed buildings and to evaluate structural damages on common
 80 infrastructures (Chou et al. 2010; Molina et al. 2012; Murphy et al., 2008; Pratt et al., 2009) or cultural
 81 heritage sites (Pollefeys et al., 2001; Manfredini et al., 2012; Koutsoudisa et al., 2014; Lazzari et al., 2017).
 82 Environmental and geological monitoring can profit from fast multi-temporal acquisitions delivering high-
 83 resolution images (Thamm and Judex 2006; Niethammer et al. 2010). RPAS can be considered a good solution
 84 also for mapping and monitoring different active processes at the earth surface (Fonstad et al., 2013; Piras
 85 et al., 2017) such as: glaciers (Immerzel et al., 2014, Ryan et al., 2015), Antarctic moss beds (Lucieer et al.,
 86 2014b), costal areas (Delacourt et al., 2009; Klemas, 2015), Interseismic deformations (Deffontaines et al.,
 87 2017), river morphodynamic (Gomez and Purdie, 2016; Jaud et al., 2016; Aicardi et al., 2017; Bolognesi et al.,
 88 2016), debri flows (Wen et al., 2011), and river channel vegetation (Dunford et al., 2009).

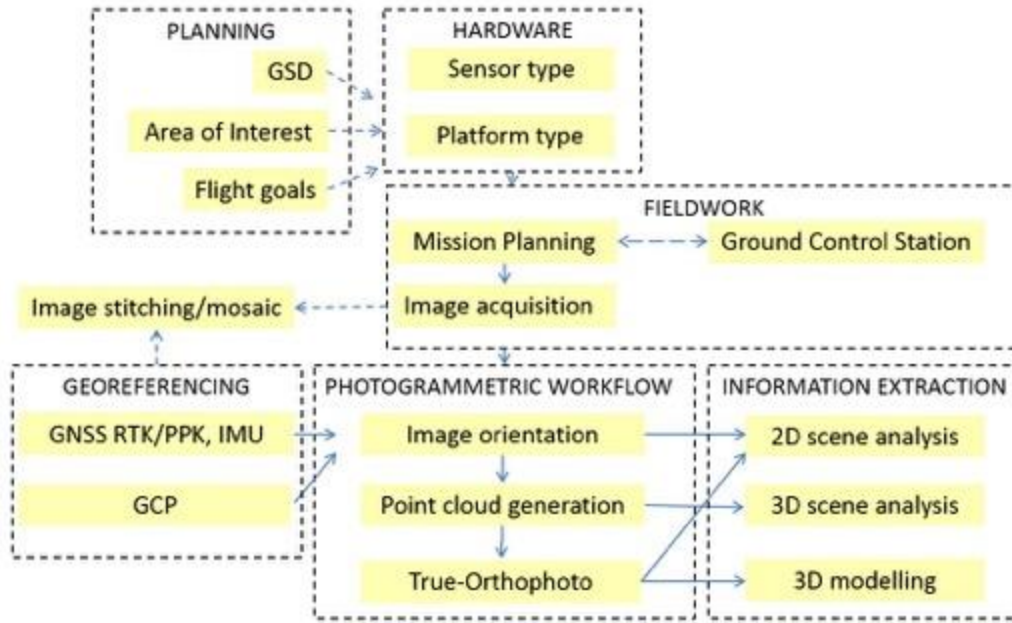
89 The incredible diffusion of RPAS has pushed many companies to develop dedicated sensors for these
 90 platforms. Besides the conventional RGB cameras other camera sensors are nowadays available on the
 91 market. Multi- and hyper-spectral cameras, as well as thermal sensors, have been miniaturized and
 92 customized to be hosted on many platforms.

93 The general workflow of a UAV acquisition is presented in Figure 2 below. The resolution of the images, the
 94 extension of the area as well as the goal of the flight are the main constraints that affect the selection of the
 95 platform and the typology of the sensor. Large areas can be flown using fixed wing (or hybrid) solutions able
 96 to acquire nadir images in a fast and efficient way. Small areas or complex objects (like steep slopes or
 97 buildings) should be acquired using rotor RPAS as they are usually slower but they allow the acquisition of
 98 oblique views. If the information different from the visible band is needed, the RPAS can host one or more
 99 sensors acquiring in different bands. The flight mission can be planned using dedicated software: they range

100 from simple apps installed on smartphones in the low-cost solutions, to laptops connected to directional
101 antennas and remote controls for the most sophisticated platforms. According to the typology of the
102 platform, different GNSS and IMU can be installed. Low-cost solutions are usually able to give positions with
103 few meters accuracy and need GCP (Ground Control Points) to geo-reference the images. On the other hand,
104 most expensive solutions install double frequency GNSS receivers with the possibility to get accurate geo-
105 referencing thanks to Real Time Kinematic (RTK) or Post Processing Kinematic (PPK) corrections. The use of
106 GCP and different GNSS solutions is a fundamental point. Gercke and Przybilla (2016) presented the effect of
107 RTK-GNSS and cross flight patterns, and Nocerino et al., (2013) presented an evaluation about RPAS
108 processing results quality considering: i) the use of GCPs, ii) different photogrammetric procedures, iii)
109 different network configurations. If a quick mapping is needed, the information delivered by the navigation
110 system can be directly used to stitch the images and produce a rough image mosaicking (Chang-chun et al.,
111 2011). In the alternative, the typical photogrammetric process is followed: (i) image orientation, (ii) DSM
112 generation and (iii) orthophoto generation. The position (geo-referencing) and the attitude (rotation towards
113 the coordinates system) of each acquisition is obtained by estimating the image orientation. In the dense
114 point cloud generation, 3D point clouds are generated from a set of images, while the orthophoto is
115 generated in the last step combining the oriented images projected on the generated point cloud, leading to
116 orthorectified images (Turner et al., 2012). Point clouds can be very often converted in Digital Surface Models
117 (DSM), and Digital Terrain Models (DTM) can be extracted removing the off ground regions (mainly buildings
118 and trees). In real applications, many parameters can influenced the final resolution of DSM/DTM and
119 ortophoto like: real GSD (Nocerino et al., 2013) interior and exterior orientation parameters (Kraft et al.,
120 2016), overlap of images, flight strip configuration and used SfM-Software (Nex et al., 2015).

121 In particular during emergencies, the time required for the image dataset processing can be a critical point.
122 For this reason, the development of fast mosaicking methods as MACS, for a real time mapping applications
123 (Lehmann et al., 2011), or VABENE++, developed by German Aerospace Center for real time traffic
124 management (Detzer et al., 2015).

125 The outputs from the last two steps (point clouds and true-orthophotos) as well as the original images are
126 very often used as input in the scene understanding process: classification of the scene or extraction of
127 features (i.e. objects) of interest using machine learning techniques are the most common applications. 3D
128 models can also be generated using the point cloud and the oriented images to texturize the model.



129

130

Figure 2. Acquisition and processing of RPAS images: general workflow.

131

In this paper, the authors present an analysis and evaluation concerning the use of RPAS as alternative monitoring technique to the traditional methods, relating to the natural hazard scenarios. The main goal is to define and test the feasibility of a set of methodologies that can be used in the monitoring and mapping activities. The study is focused in particular on the use of mini and micro RPAS systems (Table 1). The following table listed the technical specifications of these two RPAS categories, again based on the current classification by UVS (Unmanned Vehicle Systems) International. Most of the mini or micro RPAS systems available integrate a flight control system, which autonomously stabilizes these platforms and enables the remotely controlled navigation. Additionally, they can integrate an autopilot, which allows an autonomous flight based on predefined waypoints. For the monitoring and mapping applications, mini- or micro RPAS systems are very useful as cost-efficient platforms for capturing real-time close-range imagery. These platforms can reach the area of investigation and take several photos and videos from several points and different angles of view (Gomez and Kato, 2014). For mapping applications, it is also possible to use this flight control data to geo-register the captured payload sensor data like still images or video streams (Eugster and Nebiker, 2008).

145

Table 1. Classification of mini and micro UAV systems, according to UVS International.

Category	Max. Take Of Weight	Max. Flight Altitude	Endurance	Data Link Range
Mini	<30kg	150-300m	<2h	<10km
Micro	<5Kg	250m	1h	<10km

146

2. USE OF RPAS FOR NATURAL HAZARDS DETECTION AND MONITORING

147

Gomez and Purdie (2016) published a detailed analysis of the use of RPAS for hazards and disaster risk monitoring. In our paper, we focused our attention on the most dangerous natural hazards that can be analyzed using RPAS. According to the definitions used by Annual Disaster Statistical Review (Guha-Sapir et

151

152 al., 2017), the paper considers in particular: i) landslides, ii) floods iii) earthquakes v) volcanic activity vi)
153 wildfires. For each considered category of natural hazard, the paper presents a review of a large list of
154 published papers (159 papers), analyzing proposed methodologies and provided results, and underlining
155 strengths and limitations in the use of RPAS. The aims of this paper is the description of possible use of RPAS
156 in considered natural hazards, describing a general methodology for the use of these systems in different
157 contexts merging all previous published experiences.

158

159 2.1 Landslides

160 Landslides are one of the major natural hazards that produce each year enormous property damage
161 regarding both direct and indirect costs. Landslides are rock, earth or debris flows on slopes due to gravity.
162 The event can be triggered by a variety of external elements, such as intense rainfall, water level change,
163 storm waves or rapid stream erosion that cause a rapid increase in shear stress or decrease in shear strength
164 of slope-forming materials. Moreover, the pressures of increasing population and urbanization, human
165 activities such as deforestation or excavation of slopes for road cuts and building sites, etc., have become
166 important triggers for landslide occurrence. Because the factors affecting landslides can be geophysical or
167 human-made, they can occur in developed and undeveloped areas.

168 In the field of natural hazards, the use of RPAS for landslides study and monitoring represents one of the
169 most common applications. The number of papers that present case studies or possible methodologies
170 dedicated to this topic has strongly increased in last few years and now the available bibliography offers a
171 good representation of possible approaches and technical solutions.

172 When a landslide occurs, the first information to be provided is the extent of the area affected by the event
173 (figure 3). The landslide impact extent is usually done based on detailed optical images acquired after the
174 event. From these acquisitions, it is possible to derive Digital Elevation Models (DEMs) and orthophotos that
175 allow detecting main changes in geomorphological figures (Fan et al., 2017). In this scenario, the use of the
176 mini-micro RPAS is practical for small areas and optimal for landslides that often cover an area that range
177 from less than one square kilometres up to few square kilometres. Ultra-high resolution images acquired by
178 RPAS can support the definition not only of the identification of studied landslide limit, but also the
179 identification and mapping of main geomorphological features (Fiorucci et al., 2018). Furthermore, a
180 sequence of RPAS acquisitions over the time can provide useful support for the study of the gravitational
181 process evolution.

182 According to Scaioni et al. (2014), applications of remote sensing for landslides investigations can be divided
183 into three classes: i) landside recognition, classification and post-event analysis, ii) landslide monitoring, iii)
184 landslide susceptibility and hazard assessment.

185



186

187 Figure 3. Example of RPAS image of a rockslide occurred on a road. The image was acquired after the
188 rockslide occurred in 2014 in San Germano municipality (Piemonte region, NW Italy). As presented in
189 Giordan et al. (2015a), a multi-rotor of local Civil Protection Agency was used to evaluate occurred damages
190 and residual risk. RPAS images can be very useful to have a representation from a different point of view of
191 the occurred phenomena. Even not already processed using SFM applications, this dataset can be very
192 useful for decision makers to define the strategy for the management of the first phase of emergency.

193

194 2.1.1 Landslides recognition

195 The identification and mapping of landslides are usually performed after intense meteorological events that
196 can activate or reactivate several gravitational phenomena. The identification and mapping of landslides can
197 be organized in landslides event maps. Landslides event mapping is a well-known activity obtained through
198 field surveys (Santangelo et al., 2010), visual interpretation of aerial or satellite images (Brardinoni et al.,
199 2003; Ardizzone et al., 2013) combined analysis of LiDAR DTM and images (Van Den Eeckhaut et al., 2007;
200 Haneberg et al., 2008; Giordan et al., 2013; Razak et al., 2013; Niculiță et al., 2016). The use of RPAS for the
201 identification and mapping of a landslide has been described by several authors (Niethammer et al 2009;
202 Niethammer et al 2010; Rau et al., 2011; Carvajal et al., 2011; Travelletti et al., 2012; Torrero et al., 2015;
203 Casagli et al., 2017). Niethammer et al 2009 and Liu et al. (2015) showed how RPAS could be considered a
204 good solution for the acquisition of ultra-high resolution images with low-cost systems. Fiorucci et al. (2018)
205 compared the results of the landslide limit mapped using different techniques and found that satellite images
206 can be considered a good solution for the identification and map of landslides over large areas. On the
207 contrary, if the target of the study is the definition of landslide's morphological features, the use of more
208 detailed RPAS images seemed to be the better solution. As suggested by Walter et al., (2009) and Huang et
209 al., (2017) one of the most critical elements for a correct georeferencing of acquired images are the use of
210 GCPs. The in situ installation and positioning acquisition of GCPs can be an important challenge in particular
211 in dangerous areas as active landslides. Very often, GCPs are not installed in the most active part of the slide

212 but on stable areas. This solution can be safer for the operator, but it can also reduce the accuracy of the
213 final reconstruction.

214 Another parameter that can be considered during the planning of the acquisition phase is the morphology of
215 the studied area. According to with Giordan et al., (2015b), slope materials and gradient can affect the flight
216 planning and the approach used for the acquisition of the RPAS images. Two possible scenarios can be
217 identified: i) steep to vertical areas ($>40^\circ$); ii) slopes with gentle to moderate slopes ($<40^\circ$). In the first case,
218 the use of multi-copters with oblique acquisitions is often the best solution. On the contrary, with more
219 gentle slopes, the use of fixed-wing systems can assure the acquisition of wider areas.

220

221 **2.1.2 Landslides monitoring**

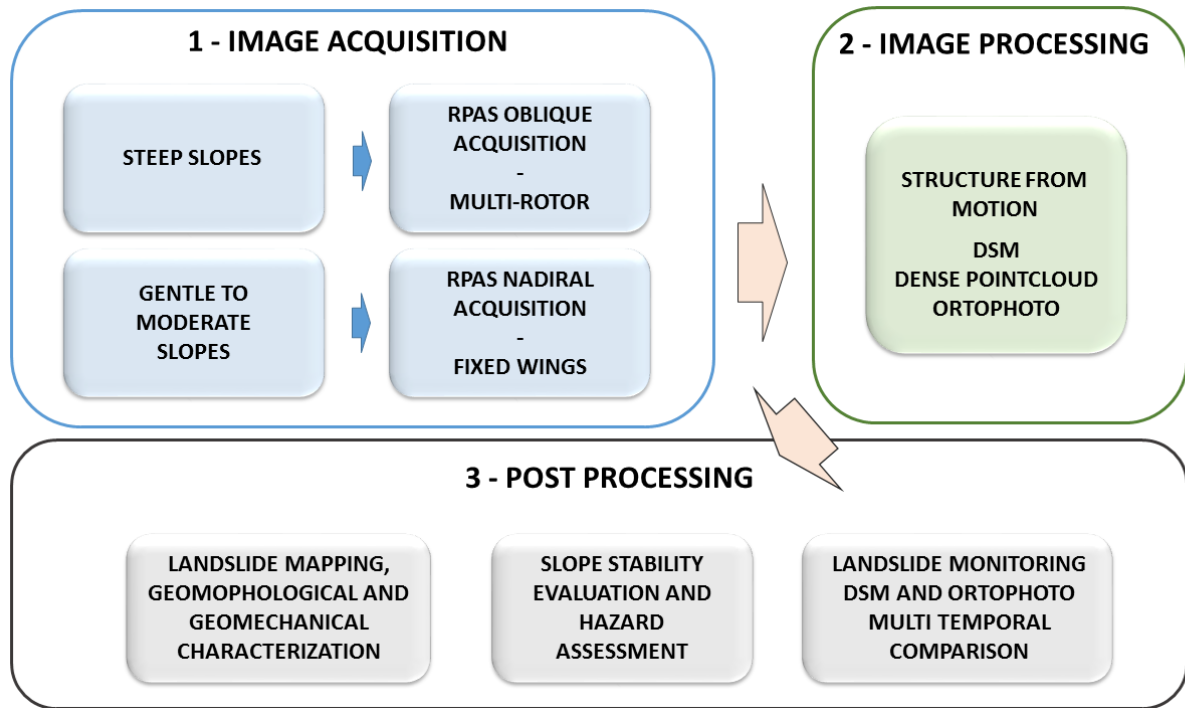
222 The second possible field of application of RPAS is the use of multi-temporal acquisitions for landslides
223 monitoring. This topic has been described by several authors (Dewitte et al., 2008; Turner and Lucieer, 2013;
224 Travelletti et al., 2012; Lucieer et al. 2014a; Turner et al., 2015; Marek et al., 2015; Lindner et al., 2016). In
225 these works, numerous techniques based on the multi-temporal comparison of RPAS datasets for the
226 definition of the evolution of landslides have been presented and discussed. Niethammer et al. (2010 and
227 2012) described how the position change of geomorphological features (in particular fissures) could be
228 considered for a multi-temporal analysis with the aim of the characterization of the landslide evolution.
229 Travelletti et al. (2012) introduced the possibility of a semi-automatic image correlation to improve this
230 approach. The use of image correlation techniques has been also described by Lucieer et al. (2014a) who
231 demonstrated that COSI-Corr (Co-registration of Optically Sensed Imaged and Correlation - Leprince et al.
232 2007, 2008; Ayoub et al., 2009) can be adopted for the definition of the surface movement of the studied
233 landslide. A possible alternative solution is the multi-temporal analysis of the use of DSMs. The comparison
234 of digital surface models can be used for the definition of volumetric changes caused by the evolution of the
235 studied landslide. The acquisition of these digital models can be done with terrestrial laser scanners (Baldo
236 et al., 2009) or airborne LiDAR (Giordan et al., 2013). Westoby et al. (2012) emphasized the advantages of
237 RPAS concerning terrestrial laser scanner, which can suffer from line-of-sight issues, and airborne LiDAR,
238 which are often cost-prohibitive for individual landslide studies. Turner et al. (2015) stressed the importance
239 of a good co-registration of multi-temporal DSM for good results that could decrease the accuracy of results.
240 The use of benchmarks in areas not affected by morphological changes can be used for a correct calibration
241 of rotational and translation parameters.

242

243 **2.1.3 Landslides susceptibility and hazard assessment**

244 Landslides susceptibility and hazard assessment are often performed at basin scale (Guzzetti et al., 2005)
245 using different remote sensing techniques (Van Westen et al., 2008). The use of RPAS can be considered for
246 single case study applications to help decision makers in the identification of the landslide damages and the
247 definition of residual risk (Giordan et al., 2015a). Saroglou et al., (2017) presented the use of RPAS for the
248 definition of trajectories of rock falls prone areas. Salvini et al. (2017) and Török et al., (2017) described the
249 combined use of TLS and RPAS for hazard assessment of steep rock walls. All these papers considered the
250 use of RPAS as a valid solution for the acquisition of DSM over sub-vertical areas. Török et al., (2017) and
251 Tannant et al., 2017 also described in their manuscripts how RPAS DSMs can be used for the evaluation of
252 slope stability using numerical modelling. Fan et al. (2017) analyzed the geometrical features and provided

253 the disaster assessment of a landslide occurred on June 24 2017 in the village of Xinmo in Maoxian County,
 254 (Sichuan Province, Southwest China). Aerial images were acquired the day after the event from an unmanned
 255 aerial vehicle (UAV) (fixed-wing UAV, with a weight less than 10 kg, and flight autonomy up to 4 hours), and
 256 a digital elevation model (DEM) was processed, with the purpose to analyzed the main landslide geometrical
 257 features (front, rear edge elevation, accumulation area, horizontal sliding distance)



258

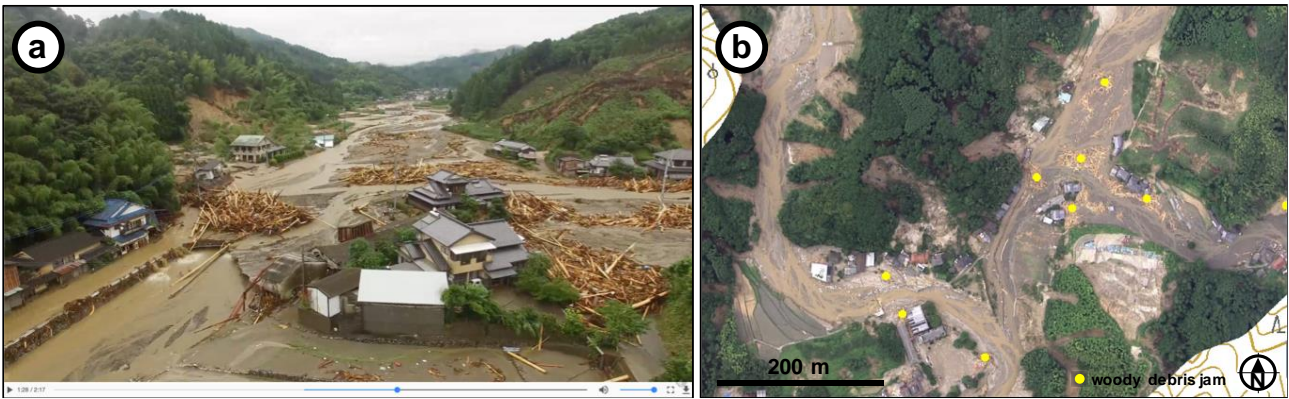
259

260 Figure 4. Acquisition, processing and post-processing of RPAS images applied to i) landslides recognition, ii)
 261 hazard assessment and iii) slope evolution monitoring.

262

263 2.2 Floods

264 Disastrous floods in urban, lowland areas often cause fatalities and severe damage to the infrastructure.
 265 Monitoring the flood flow, assessment of the flood inundation areas and related damages, post-flood
 266 landscape changes, and pre-flood prediction are therefore seriously required. Among various scales of
 267 approaches for flood hazards (Sohn et al., 2008), the RPAS has been adopted for each purpose of the flood
 268 damage prevention and mitigation because it has an ability of quick measurement at a low cost (DeBell et
 269 al., 2016; Nakamura et al., 2017). Figure 5 shows an example of the use of RPAS for prompt damage
 270 assessment by a severe flood occurred on early July 2017 at northern Kyushu area, southwest Japan. The
 271 Geospatial Information Authority of Japan (GSI) utilized an RPAS for the post-flood video recording and
 272 photogrammetric mapping of the damaged area with flood flow and large woody debris.



273

274 Figure 5. Image captures of flood hazard using RPAS just after the 2017 Northern Kyushu Heavy Rain in the
 275 early July (southwest Japan), provided by GSI. (a) A screenshot of the aerial video of a flooded area along
 276 the Akatani River, Asakura City in Fukuoka Prefecture. (b) Orthorectified image of the damaged area.
 277 Locations of woody debris jam are mapped and shown on the online map (GSI, 2017). The video and map
 278 products are freely provided (compatible with Creative Commons Attribution 4.0 International).

279

280 2.2.1. Potential analysis of flood inundation

281 The risk assessments of flood inundation before the occurrence of a flood is crucial for the mitigation of the
 282 flood-disaster damages. RPAS is capable of providing quick and detailed analysis of the land surface
 283 information including topographic, land cover, and land use data, which are often incorporated into the
 284 hydrological modelling for the flood estimate (Costa et al., 2016). As a pre-flood assessment, Li et al. (2012)
 285 explored the area around an earthquake-derived barrier lake using an integrated approach of remote sensing
 286 including RPAS for the hydrological analysis of the potential dam-break flood. They proposed a technical
 287 framework for the real-time evacuation planning by accurately identifying the source water area of the
 288 dammed lake using a RPAS, followed by along-river hydrological computations of inundation potential.
 289 Tokarczyk et al. (2015) showed that the RPAS-derived imagery is useful for the rainfall-runoff modelling for
 290 the risk assessment of floods by mapping detailed land-use information. As a key input data, high-resolution
 291 imperviousness maps were generated for urban areas from RPAS imagery, which improved the hydrological
 292 modelling for the flood assessment. Zazo et al. (2015) and Şerban et al. (2016) demonstrated hydrological
 293 calculations of the potentially flood-prone areas using RPAS-derived 3D models. They utilized 2D cross
 294 profiles derived from the 3D model for the hydrological modelling.

295

296 2.2.2. Flood monitoring

297 Monitoring of the ongoing flood is potentially important for the real-time evacuation planning. Le Coz et al.
 298 (2016) mentioned that the movies captured by a RPAS, which can be operated by not only research specialists
 299 but also general non-specialists, is potentially useful for the quantitative monitoring of floods including flow
 300 velocity estimate and flood modelling. This can also contribute to the crowdsourced data collection for flood
 301 hydrology as the citizen science. In case of flood monitoring, however, areas under water is often problematic
 302 by image-based photogrammetry because the bed is not often fully seen in aerial images. If the water is clear
 303 enough, bed images under water can be captured, and the bed morphology can be measured with additional
 304 corrections of refraction (Tamminga et al., 2015; Woodget et al., 2015), but the flood water is often unclear
 305 because of the abundant suspended sediment and disturbing flow current. Another option is the fusion of

306 different datasets using a sonar-based measurement for the water-covered area, which is registered with
307 the terrestrial datasets (Flener et al., 2013; Javernick et al., 2014). Image-based topographic data of water
308 bottom by unmanned underwater vehicle (UUV, also known as an autonomous underwater vehicle, AUV)
309 can also be another option (e.g., Pyo et al., 2015), although such the application of UUV to flooding has been
310 limited.

311 Not only the use of topographic datasets derived from Structure from Motion-Multi Stereo View (SfM-MVS)
312 photogrammetry, the use of orthorectified images concurrently derived from the RPAS-based aerial images
313 is advantageous for the assessment of hydrological observation and modelling of floods. Witek et al. (2014)
314 developed an experimental system to monitor the stream flow in real time for the prediction of overbank
315 flood inundation. The real-time prediction results are also visualized online with a web map service with a
316 high-resolution image (3 cm/pix). Feng et al. (2015) reported that the accurate identification of inundated
317 areas is feasible using RPAS-derived images. In their case, deep learning approaches of the image
318 classification using optical images and texture by RPAS successfully extracted the inundated areas, which
319 must be useful for flood monitoring. Erdelj et al. (2017) proposed a system that incorporates multiple RPAS
320 devices with wireless sensor networks to perform the real-time assessment of a flood disaster. They
321 discussed the technical strategies for the real-time flood disaster management including the detection,
322 localization, segmentation, and size evaluation of flooded areas from RPAS-derived aerial images.

323

324 **2.2.3. Post-flood changes**

325 Post-flood assessments of the land surface materials including topography, sediment, and vegetation are
326 more feasible by RPAS surveys. Smith et al. (2014) proposed a methodological framework for the immediate
327 assessment of flood magnitude and affected landforms by SfM-MVS photogrammetry using both aerial and
328 ground-based photographs. In this case, it is recommended to carefully select appropriate platforms for SfM-
329 MVS photogrammetry (either airborne or ground-based) based on the field conditions. Tamminga et al.
330 (2015) examined the 3D changes in river morphology by an extreme flood event, revealing that the changes
331 in reach-scale channel patterns of erosion and deposition are poorly modelled by the 2D hydrodynamics
332 based on the initial condition before the flood. They also demonstrate that the topographic condition can be
333 more stable after such an extreme flood event. Langhammer et al. (2017) proposed a method to
334 quantitatively evaluate the grain size distribution using optical images taken by a RPAS, which is applied to
335 the sediment structure before and after a flash flood.

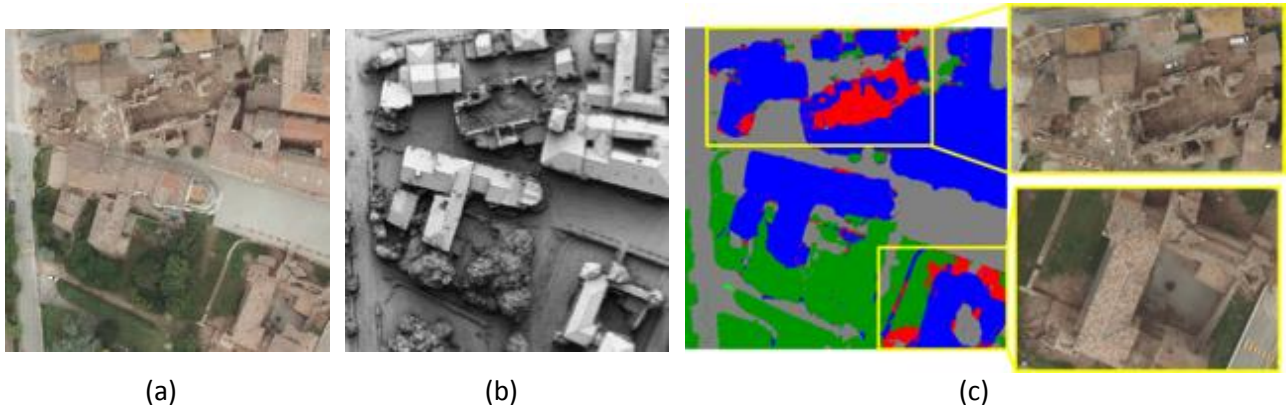
336 As a relatively long-term study, Dunford et al. (2009) and Hervouet et al. (2011) explored annual landscape
337 changes after the flood using RPAS-derived images together with other datasets such as satellite image
338 archives or a manned motor paraglider. Their work assessed the progressive development of vegetation on
339 a braided channel at an annual scale, which appears to be controlled by local climate including rainfall,
340 humidity, and air temperature, hydrology, groundwater level, topography, and seed availability. Changes in
341 the sediment characteristics by a flood is another key feature to be examined.

342

343 **2.3 Earthquakes**

344 Remote sensing technology has been recognized as a suitable source to provide timely data for automated
345 detection of damaged buildings for large areas (Dong and Shan, 2013; Pham et al., 2014). In the post-event,
346 satellite images have been traditionally used for decades to visually detect the damages on the buildings to

347 prioritize the interventions of rescuers. Operators search for externally visible damage evidence such as
348 spalling, debris, rubble piles and broken elements, which represent strong indicators of severe structural
349 damage. Several researches, however, have demonstrated how this kind of data often leads to the wrong
350 detection, usually underestimating the number of the collapsed building because of their reduced resolution
351 on the ground. In this regard, airborne images and in particular oblique acquisitions (Tu et al., 2017; Nex et
352 al., 2014; Gerke and Kerle 2011; Nedjati et al., 2016) have demonstrated to be a better input for reliable
353 assessments, allowing the development of automated algorithms for this task (Figure 6). The deployment of
354 photogrammetric aeroplanes on the strike area is however very often unfeasible especially when the early
355 (in the immediate hours after the event) damage assessment for response action is needed.



356 Figure 6. True-orthophoto, Digital Surface Model and damage map of an urban area using airborne nadir
357 images (Source: Nex et al., 2014).

358 For this reason, RPASs have turned out to be valuable instruments for the building damage assessment
359 (Hirose et al., 2015). The main advantages of RPASs are their availability (and reduced cost) and the ease to
360 repeatedly acquire high-resolution images. Thanks to their high resolution, their use is not only limited to the
361 early impact assessment for supporting rescue operations, but it is also considered in the preliminary analysis
362 of the structural damage assessment.

363

364 2.3.1 Early impact assessment

365 The fast deployment in the field, the easiness of use and the capability to provide in real time high-resolution
366 information of inaccessible areas to prioritize the operator's activities are the strongest point of RPASs for
367 these activities (Boccardo et al., 2015). The use of RPASs for rescue operations started almost a decade ago
368 (Bendea et al., 2008) but their massive adoption has begun only in the very last few years (Earthquake in
369 Nepal 2015) thanks to the development of low cost and easy to use platforms. Initiatives like *UAViators*
370 (<http://uaviators.org/>) have further increased the public awareness and acceptance of this kind of
371 instruments. Several rescue departments have now introduced RPAS as part of the conventional equipment
372 of their teams (Xie et al., 2014). The huge number of videos acquired by RPAS and posted by rescuers online
373 (i.e. Youtube) after the 2016 Italian earthquakes confirm this general trend.

374 The operators use RPASs to fly over the interest area and get information through visual assessment of the
375 streaming videos. The quality of this analysis is therefore limited to the ability of the operator to fly the RPAS
376 over the interest area. The lack of video geo-referencing usually reduces the interpretability of the scene and
377 the accurate localization of the collapsed parts: only small regions can be acquired in a single flight. The lack
378 of georeferenced maps prevents the smooth sharing of the collected information with other rescue teams

379 limiting the practical exploitation of these instruments. RPASs are mainly used in daylight conditions as the
380 flight during the night is extremely critical, and the use of thermal images is of limited help for the rescuers.

381 Many researchers have developed algorithms to automatically extract damage information from imagery
382 (Figure 7). The main focus of these works is to reliably detect damages in a reduced time to satisfy the time
383 constraints of the rescuers. In (Vetrivel et al., 2015) the combined use of images and photogrammetric point
384 clouds have shown promising results thanks to a supervised approach. This work, however, highlighted how
385 the classifier and the designed 2D and 3D features were hardly transferable to different datasets: each scene
386 needed to be trained independently strongly limiting the efficiency of this approach. In this regard, the recent
387 developments in machine learning (i.e. Convolutional Neural Networks, CNN) have overcome these limits
388 (Vetrivel et al., in press), showing how they can correctly classify scenes even if they were trained using other
389 datasets: a trained classifier can be directly used by rescuers on the acquired images without need for further
390 operations. The drawback of these techniques is the computational time: the use of CNN, processing like
391 image segmentation or point cloud generation are computationally demanding and hardly compatible with
392 real-time needs. In this regard, most recent solutions exploit only images (i.e. no need to generate point
393 cloud) and limit the use of most expensive processes to the regions where faster classification approaches
394 provide uncertain results to deliver an almost real-time information (Duarte et al., 2017).



(a)

(b)

(c)

395 Figure 7. Examples of damage detection on images acquired in three different scenarios (a) Mirabello (source: Vetrivel
396 et al., in press) and (b) L'Aquila and Lyon (source Duarte et al., 2017).

397

398 2.3.2 Building damage assessment

399 The damage evidence that can be captured from a UAV is not sufficient to infer the actual damage state of
400 the building as it requires additional information such as damages to internal building elements (e.g., columns
401 and beams) that cannot be directly defined from images. Even though this information is limited, images can
402 provide useful information about the external condition of the structure, evidencing anomalies and damages
403 and providing a first important information for structural engineers. Two main typologies of investigations
404 can be performed: (i) the use of images for the detection of cracks or damages on the external surfaces of
405 the building (i.e. walls and roofs) and (ii) the use of point clouds (generated by photogrammetric approach)
406 to detect structural anomalies like tilted or deformed surfaces. In both cases, the automated processing can
407 only support and ease the work of the expert who still interprets and assess the structural integrity of the
408 building.

409 In (Fernandez-Galarreta et al., 2015) a comprehensive analysis of both point clouds and images to support
410 the ambiguous classification of damages and their use for damage score was presented. In this paper, the

411 use of point clouds was considered efficient for more serious damages (partial or complete collapse of the
412 building), while images were used to identify smaller damages like cracks that can be used as the basis for
413 the structural engineering analysis. The use of point clouds is investigated in (Baiocchi et al., 2013; Dominici
414 et al., 2017): this contribution highlights how point clouds from UAVs can provide very useful information to
415 detect asymmetries and small deformations of the structure.

416

417 2.4 Volcanic activity

418

419 RPAS is particularly advantageous when the target area of measurement is hardly accessible on the ground
420 due to dangers of volcanic gas or risks of eruption in volcanic areas (Andrews, 2015). Although an equipment
421 of RPAS can be lost or damaged by the volcanic activities, the operator can safely stay in a remote place.
422 Various sensors can be mounted on a RPAS to monitor volcanic activities including topography, land cover,
423 heat, gas composition, and even gravity field (Saiki and Ohba, 2010; Deurloo et al., 2012; Astuti et al., 2009;
424 Middlemiss et al., 2016). The photogrammetric approach to obtain topographic data is widely applied
425 because RGB camera sensors are small enough to be mounted on a small aircraft. As mentioned before, this
426 paper considers in particular small RPAS. In the study of volcanoes, larger aircrafts with a payload of kilograms
427 are also utilized to mount other types of sensors to monitor various aspects of their dynamic activities. For
428 this reason, in this chapter we consider also larger RPAS solutions.

429

430 2.4.1. Topographic measurements of volcanoes

431 Long-distance flight of a RPAS enables quick and safe measurements of an emerging volcanic island. Tobita
432 et al. (2014a) successfully performed a fixed-wing RPAS flight for a one-way distance of 130 km in total flight
433 time of 2 hours and 51 minutes over the sea to capture aerial images of a newly formed volcanic island next
434 to Nishinoshima Island (Ogasawara Islands, southwest Pacific). They performed SfM-MVS photogrammetry
435 of the aerial images taken back from the RPAS to generate a 2.5 m resolution DEM of the island. The team
436 also performed two successive measurements of Nishinoshima Island in the following 104 days, revealing the
437 morphological changes in the new island covering a 1,600 m by 1,400 m area (Nakano et al., 2014; Tobita et
438 al., 2014b).

439 Since the volcanic activities often last for a long period, it is also important to connect the recent volcanic
440 morphological changes to those in the past. Although detailed morphological data of volcanic topography is
441 often unavailable, historical aerial photographs taken in the past decades can be utilized to generate
442 topographic models at a certain resolution. Some case studies have used archival aerial photographs in
443 volcanoes for periods of more than 60 years, generating DEMs with resolutions of several meters for areas
444 of 10 km² (Gomez, 2014; Derrien et al., 2015; Gomez et al. 2015). Although these DEMs are coarser than
445 those derived from RPAS, they can be used as supportive datasets for the modern morphological monitoring
446 using RPAS at a higher resolution and measurement frequency.

447

448 2.4.2. Gas monitoring and product sampling

449 Caltabiano et al. (2005) proposed the architecture of a RPAS for the direct monitoring of gas composition in
450 volcanic clouds of Mt. Etna in Italy. In this system, the 2-m wide fixed-wing RPAS can fly autonomously up to
451 4000 m altitude with a speed of 40 km/h. Like this system, a RPAS with a payload of several kilograms can
452 carry multiple sensors to monitor different compositions of volcanic gas. McGonigle et al. (2008) used a RPAS
453 for volcanic gas measurements at La Fossa crater of Mt. Vulcano in Italy. The RPAS has 3 kg payload and
454 allows to host an ultraviolet spectrometer, an infrared spectrometer, and an electrochemical sensor on
455 board. The combination of these sensors enabled the estimation of the flux of SO₂ and CO₂, which are crucial
456 for revealing the geochemical condition of erupting volcanoes. The monitoring of gas composition including
457 CO₂, SO₂, H₂S, H₂, as well as the air temperature, can be used for the quantification of the degassing activities
458 and prediction of the conduit magma convection, as suggested by the tests at several volcanoes in Japan
459 (Shinohara, 2013; Mori et al., 2014) and in Costa Rica (Diaz et al., 2015).

460 A RPAS can also transport a small ground-running robot (Unmanned Ground Vehicle: UGV) to slope head of
461 an active volcano, where the UGV takes close-range photographs of volcanic ash on the ground surface by
462 running down the slope (Nagatani et al., 2013). Protocols for direct sampling of volcanic products using a
463 RPAS have also been developed (Yajima et al., 2014).

464

465 **2.4.3. Geothermal monitoring**

466 In New Zealand, Harvey et al. (2016) and Nishar et al. (2016) carried out experimental studies on the regular
467 monitoring of intense geothermal environments using a small RPAS. They used thermal images taken by an
468 infrared imaging sensor together with normal RGB images for photogrammetry, mapping both the ground
469 surface temperature with detailed topography and land cover data. Chio and Lin (2017) further assessed the
470 use of a RPAS equipped with a thermal infrared sensor for the high-resolution geothermal image mapping in
471 a volcanic area in Taiwan. They improved the measurement accuracies using an onboard sensor capable of
472 post-processed kinematic GNSS positioning. This allows accurate mapping with less ground control points,
473 which are hard to place on such intense geothermal fields.

474

475 **2.5 Wildfires**

476 Wildfires are a phenomenon with local and global effects (Filizzola et al., 2017). Wildfires represent a serious
477 threat for land managers and property owners; in the last few years, this threat has significantly expanded
478 (Peters et al., 2013). The literature also suggests that climate change will continue to enhance the potential
479 forest fire activity in different regions of the world (McKenzie et al. 2014; Abatzoglou and Williams, 2016).
480 Remote sensing technologies can be very useful in monitoring such hazard (Shroeder et al., 2016). Several
481 scientists in the last few years used satellites in fire monitoring (Shroeder et al., 2016). More recently, RPASs
482 have been considered to be useful as well (Martinez-de Dios et al., 2011). Hinkley and Zajkowski (2011)
483 presented the results of a collaborative partnership between NASA, and the US Forest Service established
484 for testing thermal image data for wildfires monitoring. A small unmanned airborne system served as a sensor
485 platform. The outcome was an improved tool for wildfire decision support systems. Merino et al. (2012)
486 described a system for forest fire monitoring using a RPAS. The system integrates the information from the
487 fleet of different vehicles to estimate the evolution of the forest fire in real time. The field tests indicated
488 that RPAS could be very helpful for the activities of firefighting (e.g. monitoring). Indeed, they cover the gap
489 between the spatial scales given by satellites and those based on cameras. Wing et al. (2014) underlined the
490 fact that spectral and thermal sensors mounted in RPASs may hold great promise for future remote sensing

491 applications related to forest fires. RPASs have greater potential to provide enhanced flexibility for
492 positioning and repeated data collection. Tang and Shao (2015) summarize various approaches of remote
493 drone sensing to surveying forests, mapping canopy gaps, measuring forest canopy height, tracking forest
494 wildfires, and supporting intensive forest management. These authors underlined the usefulness in using
495 drones for wildfire monitoring. RPASs can repeatedly fly to record the extent of an ongoing wildfire without
496 jeopardizing crews' safety. Zajkowski et al. (2015) tested different RPASs (e.g. quadcopter, fixed-wing) for the
497 analysis of fire activity. Measurements included visible and long-wave infrared (LWIR) imagery, black carbon,
498 air temperature, relative humidity and three-dimensional wind speed and direction. The authors also
499 described in detail the mission's plan, including the logistics of integrating RPAS into a complex operations
500 environment, specifications of the aircraft and their measurements, execution of the missions and
501 considerations for future missions. Allison et al. (2016) provided a detailed state of the art on fire detection
502 using both manned and unmanned aerial platforms. This review highlighted the following challenges: the
503 need to development of robust automatic detection algorithms, the integration of sensors of varying
504 capabilities and modalities, the development of best practices for the use of new sensor platforms (e.g. mini
505 RPAS), and their safe and effective operation in the airspace around a fire.

506

507 **3. Discussion and conclusion**

508 In this paper, we analysed possible applications of RPAS to natural hazards. The available literature on this
509 topic is strongly increased in last few years, according to the improvement of the diffusion of these systems.
510 In particular, we considered: landslides, floods, earthquakes, volcanic activities and wildfires.

511 RPAS can support studies on active geological processes and can be considered a good solution for the
512 identification of effects and damages due to several catastrophic events. One of the most important elements
513 that characterized the use of RPAS is their flexibility and versatility, largely confirmed by the wide number of
514 operative solutions available in the literature. The available literature pointed out the necessity of the
515 development of dedicated methodologies that can be able to take the full advantage of RPAS. In particular,
516 typical results of structure from motion software (orthophoto and DSM) that are considered the end of
517 standard data-processing, can be very often the starting point of dedicated procedures specifically conceived
518 for natural hazards applications.

519 In the pre-emergency phase, one of the main advantages of RPAS surveys is to acquire high resolution and
520 low-cost data to analyse and interpret environmental characteristics and potential triggering factors (e.g.
521 slope, lithology, geostructure, land use/land cover, rock anomalies, and displacement). The data can be
522 collected with high revisit times to obtain multi-temporal observations. After the characterization of hazard
523 potential and vulnerability, some areas can be identified by a higher level of risk. These cases request an
524 intensive monitoring, to gain a quantitative evaluation of the potential occurrence of an event. In this
525 context, the use of aerial data represents a very useful complementary data source concerning the
526 information acquired through ground-based observations in particular for dangerous areas.

527 During the emergency phase, high-resolution imagery is asked to be acquired over the event site. The primary
528 use of this data is for the assessment of the damage grade (extent, type and damage grades specific to the
529 event and eventually of its evolution). They may also provide relevant information that is specific to critical
530 infrastructures, transport systems, aid and reconstruction logistics, government and community buildings,
531 hazard exposure, displaced population, etc (Ezequiel et al., 2014). Concurrently, the availability of clear and
532 straightforward raster and vector data, integrated with base cartographic contents (transportation, surface

533 hydrology, boundaries, etc.) it is recognized as an added-value to support decision makers for the
534 management of emergency operations (Fikar et al., 2016). These applications very often need prompt and
535 reliable interventions. RPAS should, therefore, deliver information promptly. In this regard, very few
536 researchers have focused on this issue: most of the reported works present (often time-consuming and even
537 manual) post-processing of the acquired data, precluding the use of their results from practical and real-life
538 scenarios. A big effort should be taken by the research community to propose faster and automated
539 approaches. In particular during emergencies, the time required for RPAS dataset processing is an important
540 element that should be carefully considered. Giordan et al. (2015a) presented a case study related to a
541 landslide emergency. In this paper, authors considered not only possible results but also the time that is
542 required for them

543 As in many other domains, RPAS present a disruptive technology where, beside conventional SfM
544 applications for 3D reconstructions, many dedicated and advanced methodologies are still in their
545 experimental phase and will need to be further developed in the incoming years. In the following years, it
546 would be desirable to witness the transfer of the best practices in the use of RPAS be then from the Research
547 community to Government Agencies (or private companies) involved in the prevention and reduction of
548 impacts of natural hazards. The Scientific community should contribute to the definition of standard
549 methodologies that can be assumed by civil protection agencies for the management of emergencies.

550 **References**

- 551 Abatzoglou, J.T. and Williams, A.P.: Impact of anthropogenic climate change on wildfire across western US
552 forests, *PNAS*, 113 (42), 11770-11775, 2016.
- 553 Astuti, \G., Giudice, G., Longo, D., Melita, C. D., Muscato, G. and Orlando, A.: An overview of the “Volcan
554 project”: An UAS for Exploration of volcanic environments, *J Intell. Robot Syst.*, 54, 471-494, 2009.
- 555 Aicardi, I., Chiabrando, F., Lingua, A., Noardo, F., Piras, M. and Vigna, B.: A methodology for acquisition and
556 processing of thermal data acquired by UAVs: a test about subfluvial springs’ investigations, *Geomatics,
557 Natural Hazards and Risk*. 8:1, 5-17, 2017. DOI: 10.1080/19475705.2016.1225229
- 558 Allison R.S., Johnston J.M., Craig G. and Jennings S.: Airborne Optical and Thermal Remote Sensing for
559 Wildfire Detection and Monitoring Sensors, 16(8), 1310, doi:10.3390/s16081310, 2016
- 560 Andrews, C.: Pressure in the danger zone [volcanoes], *Eng. Technol.*, 10(7), 56–61, doi:10.1049/et.2015.0720,
561 2015.
- 562 Ardizzone, F., Fiorucci, F., Santangelo, M., Cardinali, M., Mondini, A.C., Rossi, M., Reichenbach, P., and
563 Guzzetti, F.: Very-high resolution stereoscopic satellite images for landslide mapping. C. Margottini, P. Canuti,
564 K. Sassa (Eds.), *Landslide Science and Practice, Landslide Inventory and Susceptibility and Hazard Zoning*, 1,
565 Springer, Heidelberg, Berlin, New York, 95–101, https://doi.org/10.1007/978-3-642-31325-7_12, 2013.
- 566 Ayoub, F., LePrince, S. and Keene, L.: User’s Guide to Cosis-Corr: Co-Registration of Optically Sensed Images
567 and Correlation; California Institute of Technology: Pasadena, CA, USA, pp. 38, 2009.
- 568 Baldo M., Bicocchi C., Chiocchini U., Giordan D. and Lollino G.: LIDAR monitoring of mass wasting processes:
569 The Radicofani landslide, Province of Siena, Central Italy, *Geomorphology*, 105, 193-201, doi:
570 10.1016/j.geomorph.2008.09.015, 2009.
- 571 Baiocchi, V., Dominici, D. and Mormile, M.: UAV application in post-seismic environment”, *International
572 Archives of the Photogrammetry, Remote Sensing and Spatial Information Sciences*, Volume XL-1/W2, UAV-
573 g2013, 4 – 6 September 2013, Rostock, Germany, pp. 21-25, 2013.
- 574 Bendea, H., Boccardo, P., Dequal, S., Tondo, G., Marenchino, D. and Piras, M.: Low cost UAV for post-disaster
575 assessment. *Int. Arch. Photogramm. Remote Sens. Spat. Inf. Sci.*, 37, 1373–1379, 2008.
- 576 Boccardo, P., Chiabrando, F., Dutto, F., Tonolo, F.G. and Lingua, A.: UAV deployment exercise for mapping
577 purposes: Evaluation of emergency response applications, *Sensors*, 15(7), 15717-15737, 2015.
- 578 Bolognesi, M., Farina, G., Alvisi, S., Franchini, M., Pellegrinelli, A. and Russo, P.: Measurement of surface
579 velocity in open channels using a lightweight remotely piloted aircraft system. *Geomatics, Natural Hazards
580 and Risk*, 8:1, 73.86, 2016. DOI: 10.1080/19475705.2016.1184717
- 581 Brardinoni, F., Slaymaker, O., and Hassan, M.A.: Landslides inventory in a rugged forested watershed: a
582 comparison between air-photo and field survey data, *Geomorphology*, 54, 179-196,
583 [https://doi.org/10.1016/S0169-555X\(02\)00355-0](https://doi.org/10.1016/S0169-555X(02)00355-0), 2003.
- 584 Brostow, G.J., Shotton, J., Fauqueur, J. and Cipolla, R.: Segmentation and Recognition Using Structure from
585 Motion Point Clouds. *Proc. 10th European Conf. on Computer Vision: Part I*, 44–57, doi:10.1007/978-3-540-
586 88682-2_5, 2008

587 Caltabiano, D., Muscato, G., Orlando, A., Federico, C., Giudice, G. and Guerrieri, S.: Architecture of a UAV for
588 volcanic gas sampling, in 2005 IEEE Conference on Emerging Technologies and Factory Automation, 1, 739-
589 744, 2005.

590 Carvajal, F., Agüera, F. and Pérez, M.: Surveying a landslide in a road embankment using Unmanned Aerial
591 Vehicle photogrammetry, *ISPRS Arch.*, 38, 1-6, 2011.

592 Casagli N., Frodella, W., Morelli, S., Tofani, V., Ciampalini, A., Intrieri, E., Raspini, F., Rossi, G., Tanteri, L. and
593 Lu, P.: Spaceborne, UAV and ground-based remote sensing techniques for landslide mapping, monitoring and
594 early warning, *Geoenvironmental Disasters*, 4(9), 1-23, DOI 10.1186/s40677-017-0073-1, 2017.

595 Chang-Chun L., Zhang, G., Lei, T. and Gong, A.: Quick image-processing method of UAV without control points
596 data in earthquake disaster area. *Transactions of Nonferrous Metals Society of China*, 21(3), s523-s528, 2011.

597 Chio, S.-H. and Lin, C.-H.: Preliminary Study of UAS Equipped with Thermal Camera for Volcanic Geothermal
598 Monitoring in Taiwan, *Sensors*, 17(7), 1649, doi:10.3390/s17071649, 2017.

599 Costa, D., Burlando, P. and Priadi, C.: The importance of integrated solutions to flooding and water quality
600 problems in the tropical megacity of Jakarta, *Sustain. Cities Soc.*, 20, 199–209, doi:10.1016/j.scs.2015.09.009,
601 2016.

602 Filizzola, C., Corrado, R., Marchese, F., Mazzeo, G., Paciello, R., Pergola, N. and Tramutoli, V.: RST-FIRES, an
603 exportable algorithm for early-fire detection and monitoring: Description, implementation, and field
604 validation in the case of the MSG-SEVIRI sensor, *Remote Sensing of Environment* Volume, 192, 2-25, 2017.

605 Chou, T.Y., Yeh, M.L., Chen, Y. and Chen, Y.H.: Disaster monitoring and management by the unmanned aerial
606 vehicle technology. *Int. Archives of Photogrammetry, Remote Sensing and Spatial Information*
607 *Sciences*, 38(7B), 137-142, 2010.

608 DeBell, L., Anderson, K., Brazier, R. E., King, N. and Jones, L.: Water resource management at catchment scales
609 using lightweight UAVs: current capabilities and future perspectives, *J. Unmanned Veh. Syst.*, 4(1), 7–30,
610 doi:10.1139/juvs-2015-0026, 2016.

611 Deffontaines, B., Chang, K.J., Champenois, J., Fruneau, B., Pathier, E., Hu, J.C., Lu, S.T. and Liu Y.C.: Active
612 interseismic shallow deformation of the Pingting terraces (Longitudinal Valley – Eastern Taiwan) from UAV
613 high-resolution topographic data combined with InSAR time series. *Geomatics, Natural Hazards and Risk*,
614 8(1), 120-136, 2017.

615 Delacourt, C., Allemand, P., Jaud, M., Grandjean, P., Deschamps, A., Ammann, J., Cuq, V. and Suanez, S.:
616 DRELIO: An Unmanned Helicopter for Imaging Coastal Areas. *J. Coast. Res.* 56, 1489-1493, 2009.

617 Derrien, A., Villeneuve, N., Peltier, A. and Beauducel, F.: Retrieving 65 years of volcano summit deformation
618 from multitemporal structure from motion: The case of Piton de la Fournaise (La Réunion Island), *Geophys.*
619 *Res. Lett.*, 42(17), 6959–6966, doi:10.1002/2015GL064820, 2015.

620 Deurloo, R., Bastos, L. and Bos, M.: On the Use of UAVs for Strapdown Airborne Gravimetry, pp. 255–261,
621 Springer, Berlin, Heidelberg., 2012.

622 Detzer, S., Weber, M., Touko Tcheumadjeu, L.C., Kuhns, G. and Kendziorra A.: Decision support for
623 multimodal transportation systems at major events and disasters: a case study in the region of Brunswick

- 624 (Germany). Sener S.M., Brebbia C.A. and Ozcevik O (eds) Disaster management and Human Health Risk IV.
625 WIT Press, Southampton, UK, 315-326, 2015.
- 626 Dewitte, O., J.C. Jasselette, Y. Cornet, M. Van Den Eeckhaut, A. Collignon, J. Poesen, and A. Demoulin.:
627 Tracking landslide displacements by multitemporal DTMs: A combined aerial stereophotogrammetric and
628 LIDAR approach in western Belgium. *Engineering Geology*, 7, 582–586, 2008.
- 629 Diaz, J. A., Pieri, D., Wright, K., Sorensen, P., Kline-Shoder, R., Arkin, C. R., Fladeland, M., Bland, G.,
630 Buongiorno, M. F., Ramirez, C., Corrales, E., Alan, A., Alegria, O., Diaz, D. and Linick, J.: Unmanned Aerial Mass
631 Spectrometer Systems for In-Situ Volcanic Plume Analysis, *J. Am. Soc. Mass Spectrom.*, 26(2), 292–304,
632 doi:10.1007/s13361-014-1058-x, 2015.
- 633 Dominici, D., Alicandro, M., Massimi, V.: UAV photogrammetry in the post-earthquake scenario: case studies
634 in L'Aquila. *Geomatics, Natural Hazards and Risk*, 8(1), 87-103, 2017.
- 635 Dong, L., Shan, J.: A comprehensive review of earthquake-induced building damage detection with remote
636 sensing techniques. *ISPRS Journal of Photogrammetry and Remote Sensing*, 84, pp. 85-99, 2013.
- 637 Duarte, D., Nex, F., Kerle, N., Vosseman, G.: Towards a more efficient detection of earthquake induced facad
638 damages using oblique UAV imagery. *International Archives of the Photogrammetry, Remote Sensing and*
639 *Spatial Information Sciences*. To be published. 2017.
- 640 Dunford, R., Michel, K., Gagnage, M., Piégay, H. and Trémelo M.-L.: Potential and constraints of Unmanned
641 Aerial Vehicle technology for the characterization of Mediterranean riparian forest, *International Journal of*
642 *Remote Sensing*, 30, 4915-4935, 2009.
- 643 Erdelj, M., Król, M. and Natalizio, E.: Wireless Sensor Networks and Multi-UAV systems for natural disaster
644 management, *Comput. Networks*, 124, 72–86, doi:10.1016/j.comnet.2017.05.021, 2017.
- 645 Eugster, H. and Nebiker, S.: UAV-based augmented monitoring– real-time georeferencing and integration of
646 video imagery with virtual globes. In: *Int. Archives of Photogrammetry, Remote Sensing and Spatial*
647 *Information Sciences*, Beijing, China, 37(B1), 1229–1235. 2008.
- 648 Ezequiel, C.A.F., Cua, M., Libatiquem, N.C., Tangonan, G.L., Alampay, R., Labuguen, R.T., Favila, C.M.,
649 Honrado, J.L.E., Canos, V., Devaney, C., Loreto, L.B., Bacusmo, J. and Palma, B.: UAV Aerial Imaging
650 Applications for Post-Disaster Assessment, Environmental Management and Infrastructure Development.
651 2014 International Conference on Unmanned Aircraft Systems (ICUAS) Orlando, FL, USA proceedings: 274–
652 283, 2014.
- 653 Fan, J., Zhang, X., Su, F., Ge, Y., Tarolli, P., Yang, Z., Zeng, C., and Zeng, Z.: Geometrical feature analysis and
654 disaster assessment of the Xinmo landslide based on remote sensing data, *Journal of Mountain Science*, 14,
655 1677–1688, doi:10.1007/s11629-017-4633-3, 2017.
- 656 Feng, Q., Liu, J. and Gong, J.: Urban Flood Mapping Based on Unmanned Aerial Vehicle Remote Sensing and
657 Random Forest Classifier—A Case of Yuyao, China, *Water*, 7(4), 1437–1455, doi:10.3390/w7041437, 2015.
- 658 Fernandez Galarreta, J., Kerle, N. and Gerke, M. UAV - based urban structural damage assessment using
659 object - based image analysis and semantic reasoning. *Natural hazards and earth system sciences*, 15(6) pp.
660 1087-1101, 2015.

661 Fikar, C., Gronalt, M., and Hirsch, P.A.: decision support system for coordinated disaster relief distribution.
662 *Exp. Syst. Appl.* 57, 104–116. doi:10.1016/j.eswa.2016.03.039, 2016.

663 Filizzola, C., Corrado, R., Marchese, F., Mazzeo, G., Paciello, R., Pergola, N. and Tramutoli, V.: RST-FIRES, an
664 exportable algorithm for early-fire detection and monitoring: Description, implementation, and field
665 validation in the case of the MSG-SEVIRI sensor, *Remote Sensing of Environment*, 192, 2-25, 2017.

666 Fiorucci, F., Giordan, D., Santangelo, M., Dutto, F., Rossi, M., and Guzzetti, F.: Criteria for the optimal selection
667 of remote sensing images to map event landslides, *Nat. Hazards Earth Syst. Sci.*, 18, 405-417, 2018.

668 Flener, C., Vaaja, M., Jaakkola, A., Krooks, A., Kaartinen, H., Kukko, A., Kasvi, E., Hyyppä, H., Hyyppä, J. and
669 Alho, P.: Seamless mapping of river channels at high resolution using mobile LiDAR and UAV-photography,
670 *Remote Sens.*, 5(12), 6382–6407, doi:10.3390/rs5126382, 2013.

671 Fonstad, M.A., Dietrich, J.T., Courville, B.C., Jensen J.L. and Carbonneau, P.E.: Topographic structure from
672 motion: a new development in photogrammetric measurement, *Earth Surf. Process. Landforms*, 38, 421-430,
673 2013.

674 Gerke, M. and Przybilla, H.J.: Accuracy analysis of photogrammetric UAV image blocks: Influence of on-board
675 RTK-GNSS and cross flight patterns, *Photogrammetrie-Fernerkundung-Geoinformation* 2016 (1), 17-30, 2016.

676 Gerke, M. and Kerle, N.: Automatic structural seismic damage assessment with airborne oblique pictometry
677 imagery. In: *PE&RS = Photogrammetric Engineering and Remote Sensing*, 77(9) pp. 885-898, 2011.

678 Giordan, D., Allasia, P., Manconi, A., Baldo, M., Santangelo, M., Cardinali, M., Corazza, A., Albanese, V.,
679 Lollino, G., and Guzzetti, F.: Morphological and kinematic evolution of a large earthflow: The Montaguto
680 landslide, southern Italy, *Geomorphology*, 187, 61-79, 2013.

681 Giordan, D., Manconi, A., Facello, A., Baldo, M., dell'Anese, F., Allasia, P. and Dutto, F.: Brief Communication
682 "The use of UAV in rock fall emergency scenario", *Nat. Hazards Earth Syst. Sci.*, 15, 163-169, 2015a.

683 Giordan, D., Manconi, A., Tannant, D. and Allasia, P.: UAV: low-cost remote sensing for high-resolution
684 investigation of landslides. *IEEE International Symposium on Geoscience and Remote Sensing IGARSS*, 26-31
685 July 2015, Milan, Italy, 5344-5347, 2015b.

686 Giordan, D., Notti, D., Villa, A., Zucca, F., Calò, F., Pepe, A., Dutto, F., Pari, p., Baldo, M. and Allasia, P.: Low
687 cost, multiscale and multi-sensor application for flooded areas mapping. *Nat. Hazards Earth Syst. Sci.*
688 *Discuss.* <https://doi.org/10.5194/nhess-2017-420>, 2017

689 Gomez, C.: Digital photogrammetry and GIS-based analysis of the bio-geomorphological evolution of
690 Sakurajima Volcano, diachronic analysis from 1947 to 2006, *J. Volcanol. Geotherm. Res.*, 280, 1–13,
691 doi:10.1016/j.jvolgeores.2014.04.015, 2014.

692 Gomez, C. and Kato, A.: Multi-scale voxel-based algorithm for UAV-derived point-clouds of complex surfaces.
693 *IEEE International ICARES – Aerospace Electronics and Remote Sensing Technology*: 205–209. 2014.

694 Gomez, C. and Purdie, H.: UAV- based Photogrammetry and Geocomputing for Hazards and Disaster Risk
695 Monitoring – A Review. *Geoenvironmental Disasters* 3(23), 1-11, 2016.

696 Gomez, C., Hayakawa, Y. and Obanawa, H.: A study of Japanese landscapes using structure from motion
697 derived DSMs and DEMs based on historical aerial photographs: New opportunities for vegetation monitoring
698 and diachronic geomorphology, *Geomorphology*, 242, 11–20, doi:10.1016/j.geomorph.2015.02.021, 2015.

699 GSI: Information on the 2017 Northern Kyushu Heavy Rain, Geospatial Inf. Auth. Japan [online] Available
700 from: http://www.gsi.go.jp/BOUSAI/H29hukuoka_ooita-heavyrain.html (Accessed 16 September 2017),
701 2017.

702 Guha-Sapir, D., Hoyois, P., Wallemacq P. and Below, R.: Annual Disaster Statistical Review 2016 The
703 numbers and trends. Centre for Research on the Epidemiology of Disasters, Ciaco Imprimerie, Louvain-la-
704 Neuve (Belgium), pp. 91, 2017.

705 Guzzetti, F., Reichenbach, P., Cardinali, M., Galli, M. and Ardizzone, F.: Probabilistic landslide hazard
706 assessment at the basin scale, *Geomorphology*, 72(1-4), 272-299, 2005.

707 Haneberg, W. C.: Using close range terrestrial digital photogrammetry for 3-D rock slope modeling and
708 discontinuity mapping in the United States, *Bulletin of Engineering Geology and the Environment*, 67(4), 457-
709 469, 2008.

710 Harvey, M. C., Rowland, J. V. and Luketina, K. M.: Drone with thermal infrared camera provides high
711 resolution georeferenced imagery of the Waikite geothermal area, New Zealand, *J. Volcanol. Geotherm. Res.*,
712 325, 61–69, doi:10.1016/j.jvolgeores.2016.06.014, 2016.

713 Hervouet, A., Dunford, R., Piégay, H., Belletti, B. and Trémélo, M.-L.: Analysis of Post-flood Recruitment
714 Patterns in Braided-Channel Rivers at Multiple Scales Based on an Image Series Collected by Unmanned Aerial
715 Vehicles, Ultra-light Aerial Vehicles, and Satellites, *GIScience Remote Sens.*, 48(1), 50–73, doi:10.2747/1548-
716 1603.48.1.50, 2011.

717 Hinkley, E. and Zajkowski, T.: USDA forest service-NASA: unmanned aerial systems demonstrations—pushing
718 the leading edge in fire mapping, *Geocarto Int.*, 26(2), 103-111, 2011.

719 Hirose, M., Xiao, Y., Zuo, Z., Kamat, V. R., Zekkos, D. and Lynch, J.: Implementation of UAV localization
720 methods for a mobile post-earthquake monitoring system, in 2015 IEEE Workshop on Environmental, Energy,
721 and Structural Monitoring Systems (EESMS) Proceedings, pp. 66–71, IEEE., 2015.

722 Huang H., Long J., Lin H., Zang L., Yi W. and Lei B.: Unmanned aerial vehicle based remote sensing method for
723 monitoring a steep mountainous slope in the Three Gorges Reservoir, China, *Earth Science Informatics* 10 (3)
724 287-301, 2017.

725 Immerzeel, W.W., Kraaijenbrink, P. D. A., Shea, J. M., Shrestha, A. B., Pellicciotti, F., Bierkens, M. F. P. and de
726 Jonga, .S.M.: High-resolution monitoring of Himalayan glacier dynamics using unmanned aerial vehicles,
727 *Remote Sensing of Environment*, 150, 93-103, 2014.

728 Jaud, M.; Grasso, F.; Le Dantec, N.; Verney, R.; Delacourt, C.; Ammann, J.; Deloffre, J.; Grandjean, P. Potential
729 of UAVs for Monitoring Mudflat Morphodynamics (Application to the Seine Estuary, France). *ISPRS Int. J. Geo-
730 Inf.* 5(4), 50, 2016.

731 Javernick, L., Brasington, J. and Caruso, B.: Modeling the topography of shallow braided rivers using Structure-
732 from-Motion photogrammetry, *Geomorphology*, 213, 166–182, doi:10.1016/j.geomorph.2014.01.006, 2014.

- 733 Joyce K. E., Belliss, S. E., Samsonov, S. V., McNeill, S. J. and Glassey, P. J.: A review of the status of satellite
734 remote sensing and image processing techniques for mapping natural hazards and disasters. *Progress in*
735 *Physical Geography*, 33, 83-207, 2009.
- 736 Kraft, T., Geßner, M., Meißner, H., Cramer, M., Gerke, M. and Przybilla, H.J.: Evaluation of a metric camera
737 system tailored for high precision UAV applications. In: *Proceedings of the XXIII ISPRS Congress : From human*
738 *history to the future with spatial information*, 12-19 July 2016, Prague, Czech Republic. Peer reviewed *Annals,*
739 *Volume III-2*, 2016. Comm II, ThS14 recent developments in Open Data - Prague. Vol. XLI-B1, ISSN 2194-9034,
740 2016
- 741 Klemas, V. V.: Coastal and Environmental Remote Sensing from Unmanned Aerial Vehicles: An Overview,
742 *Journal of Coastal Research*, 31(5), 1260-1267, 2015.
- 743 Koutsoudisa, A., Vidmarb, B., Ioannakisa, G., Arnaoutogloua, F., Pavlidis, V. and Chamzasc, C.: Multi-image
744 3D reconstruction data evaluation, *Journal of Cultural Heritage*, 15, 73-79, 2014.
- 745 Lazzari, M. and Gioia D.: UAV images and high-resolution DEMs for geomorphological analysis and hazard
746 evaluation: the case of the Uggiano archaeological site (Ferrandina, southern Italy). *Geomatics, Natural*
747 *Hazards and Risk*, 8(1), 104-119, 2017.
- 748 Langhammer, J., Lendzioch, T., Miřijovský, J. and Hartvich, F.: UAV-based optical granulometry as tool for
749 detecting changes in structure of flood depositions, *Remote Sens.*, 9(3), doi:10.3390/rs9030240, 2017.
- 750 Le Coz, J., Patalano, A., Collins, D., Guillén, N. F., García, C. M., Smart, G. M., Bind, J., Chiaverini, A., Le
751 Boursicaud, R., Dramais, G. and Braud, I.: Crowdsourced data for flood hydrology: Feedback from recent
752 citizen science projects in Argentina, France and New Zealand, *J. Hydrol.*, 541, 766–777,
753 doi:10.1016/j.jhydrol.2016.07.036, 2016.
- 754 Lehmann, F., Berger, R., Brauchle, J. Hein, D., Meißner H. and Pless, S.: MACS - Modular Airborne Camera
755 System for generating photogrammetric high-resolution products. *Zeitschrift der Deutschen Gesellschaft für*
756 *Geowissenschaften*, Schweizerbart Science Publishers, Stuttgart, Germany, (6), pp. 435-446, 2011
- 757 Leprince, S., Berthier, E., Ayoub, F., Delacourt, C. and Avouac, J.-P.: Monitoring Earth Surface Dynamics With
758 Optical Imagery, *Eos, Trans. Am. Geophys. Union*, 89(1), 1–2, doi:10.1029/2008EO010001, 2008.
- 759 Leprince, S., Barbot, S., Ayoub, F. and Ayouac, J.P.: Automatic and precise orthorectification, co-registration,
760 and sub-pixel correlation of satellite images, application to ground deformation measurements. *IEEE Trans.*
761 *Geosci. Remote Sens.* 46, 1529-1558, 2007.
- 762 Li, Y., Gong, J. H., Zhu, J., Ye, L., Song, Y. Q. and Yue, Y. J.: Efficient dam break flood simulation methods for
763 developing a preliminary evacuation plan after the Wenchuan Earthquake, *Nat. Hazards Earth Syst. Sci.*,
764 12(1), 97–106, doi:10.5194/nhess-12-97-2012, 2012.
- 765 Lindner, G., Schraml, K., Mansberger, R. and Hubl J.: UAV monitoring and documentation of a large landslide.
766 *Appl Geomat*, 8(1), 1-11, 2016.
- 767 Liu, C.-C., Chen, P.-L., Tomoya, M., Chen, C.-Y.: Rapidly responding to landslides and debris flow events using
768 a low-cost unmanned aerial vehicle. *J. Rem. Sens.* 9(1), 1-11, doi:10.1117/1.JRS.9.096016, 2015.

- 769 Lucieer, A., de Jong S. M. and Turner, D.: Mapping landslide displacements using Structure from Motion (SfM)
770 and image correlation of multi-temporal UAV photography, *Progress in Physical Geography*, 38(1), 97–116,
771 2014a.
- 772 Lucieer, A., Turner, D., King, D. H. and Robinson, S. A.: Using an Unmanned Aerial Vehicle (UAV) to capture
773 microtopography of Antarctic moss beds. *International Journal of Applied Earth Observation and*
774 *Geoinformation*. 27(a), 53–62, 2014b.
- 775 Manferdini, A.M.: A Methodology for the Promotion of Cultural Heritage Sites Through the Use of Low-Cost
776 Technologies and Procedures. In: *proc. 17th Int. Conf. on 3D Web Technology Los Angeles, CA, August 4-5,*
777 *2012*, 180, 2012.
- 778 Martin, P. G., Smith, N. T., Yamashiki, Y., Payton, O. D., Russell-Pavier F. S., Fardoulis, J. S., Richards D. A. and
779 Scott T. B.: 3D unmanned aerial vehicle radiation mapping for assessing contaminant distribution and
780 mobility, *International Journal of Applied Earth Observation and Geoinformation*, 52, 12-19, 2016.
- 781 Marek, L., Miřijovský, J. and Tuček, P.: Monitoring of the Shallow Landslide Using UAV Photogrammetry and
782 Geodetic Measurements, In: Lollino G., Giordan D., Crosta G.B., Corominas J., Azzam R. Wasowski J., Sciarra
783 N. (eds.) *Engineering Geology for Society and Territory – Landslide Processes*, Springer International
784 Publishing Switzerland, 2, 113-116, 2015.
- 785 Martinez-de Dios, J.R., Merino, L., Caballero, F. and Ollero, A.: Automatic forest-fire measuring using ground
786 stations and unmanned aerial systems. *Sensors*, 11(6), 6328-6353, 2011.
- 787 McKenzie, D., Shankar, U., Keane, R. E., Stavros, E. N., Heilman, W. E., Fox, D. G. and Riebau, A. C.: Smoke
788 consequences of new wildfire regimes driven by climate change, *Earth's Future*, 2(2), 35-59, 2014.
- 789 Merino, L., Caballero, F., Martínez-de-Dios, J.R., Iván, M. and Aníbal, O.: An unmanned aircraft system for
790 automatic forest fire monitoring and measurement, *J. Intell. Rob. Syst.*, 65(1-4), 533-548, 2012.
- 791 McGonigle, A. J. S., Aiuppa, A., Giudice, G., Tamburello, G., Hodson, A. J. and Gurrieri, S.: Unmanned aerial
792 vehicle measurements of volcanic carbon dioxide fluxes, *Geophys. Res. Lett.*, 35(6), 3–6,
793 doi:10.1029/2007GL032508, 2008.
- 794 Middlemiss, R.P., Samarelli, A., Paul, D.J., Hough, J., Rowan, S. and Hammond, G.D.: The First Measurement
795 of the Earth Tides with a MEMS Gravimeter, *Nature*, 531(1), 614, 2016.
- 796 Molina, P., Colomina, I., Vitoria, T., Silva, P.F., Skaloud, J., Kornus, W., Prades, R. and Aguilera, C.: Searching
797 lost people with UAVs: the system and results of the close-search project. *International Archives of the*
798 *Photogrammetry, Remote Sensing and Spatial Information Sciences*, 39(B1), 441-446, 2012.
- 799 Mori, T., Hashimoto, T., Terada, A., Yoshimoto, M., Kazahaya, R., Shinohara, H. and Tanaka, R.: Volcanic plume
800 measurements using a UAV for the 2014 Mt. Ontake eruption, *Earth, Planets Sp.*, 68(1), 49,
801 doi:10.1186/s40623-016-0418-0, 2016.
- 802 Murphy, R. R., Steimle, E., Griffin, C., Cullins, C., Hall, M. and Pratt, K.: Cooperative use of unmanned sea
803 surface and micro aerial vehicles at Hurricane Wilma, *Journal of Field Robotics*, 25(3), 164-180, 2008.

804 Nakamura, F., Shimatani, Y., Nishihiro, J., Ohtsuki, K., Itsukushima, R. and Yamada, H.: Report on flood
805 disaster in Kinu River, occurred in September, 2015 (in Japanese with English abstract), *Ecol. Civ. Eng.*, 19(2),
806 259–267, doi:10.3825/ece.19.259, 2017.

807 Nagatani, K., Akiyama, K., Yamauchi, G., Otsuka, H., Nakamura, T., Kiribayashi, S., Yoshida, K., Hada, Y., Yuta,
808 S., Fujino, K., Izu, T. and Mackay, R.: Volcanic ash observation in active volcano areas using teleoperated
809 mobile robots - Introduction to our robotic-volcano-observation project and field experiments, in: *proc. 2013*
810 *IEEE International Symposium on Safety, Security, and Rescue Robotics (SSRR)*, Linkoping, Sweden, 21-26 Oct.
811 2013, 1–6, 2013.

812 Nakano, T., Kamiya, I., Tobita, M., Iwahashi, J. and Nakajima, H.: Landform monitoring in active volcano by
813 UAV and SFM-MVS technique, *Int. Arch. Photogramm. Remote Sens. Spat. Inf. Sci. - ISPRS Arch.*, 40(8), 71–
814 75, 2014.

815 Nedjati, A., Vizvari, B., Izbirak, G.: Post-earthquake response by small UAV helicopters, *Nat. Hazards* 80, 1669–
816 1688, 2016. Doi: <http://dx.doi.org/10.1007/s11069-015-2046-6>

817 Nex, F., Gerke, M., Remondino, F., Przybilla H.-J., Bäumker, M. and Zurhorst, A.: ISPRS Benchmark for Multi-
818 Platform Photogrammetry. *ISPRS Annals of the Photogrammetry, Remote Sensing and Spatial Information*
819 *Sciences*, Vol. II3/W4, 135-142, 2015.

820 Nex, F. and Remondino, F.: UAV for 3D mapping applications: a review, *Appl. Geomatics*, 6(1), 1–15,
821 doi:10.1007/s12518-013-0120-x, 2014.

822 Nex, F., Rupnik, E., Toschi, I., Remondino, F. Automated processing of high resolution airborne images for
823 earthquake damage assessment. In: *International Archives of Photogrammetry and Remote Sensing and*
824 *Spatial Information Sciences*, Vol. XL-1, 2014

825 Niculiță, M.: Automatic landslide length and width estimation based on the geometric processing of the
826 bounding box and the geomorphometric analysis of DEMs, *Nat. Hazards Earth Syst. Sci.*, 16, 2021-2030,
827 <https://doi.org/10.5194/nhess-16-2021-2016>, 2016.

828 Niethammer, U., James, M.R., Rothmund, S., Travelletti, J. and Joswig, M.: UAV-based remote sensing of the
829 Super-Sauze landslide: evaluation and results, *Eng Geol*, 128, 2-11, 2012.

830 Niethammer, U., Rothmund, S., James, M.R., Travelletti, J. and Joswig, M.: UAV-based remote sensing of
831 landslides. In *Proceedings of the International Archives of Photogrammetry, Remote Sensing and Spatial*
832 *Information Sciences*, Commission V Symposium, Newcastle upon Tyne, UK, 21–24 June 2010, 496–501,
833 2010.

834 Niethammer, U., Rothmund, S., Joswig, M.: UAV-based remote sensing of the slow-moving landslide Super-
835 Sauze. In: Malet, J.-P., Remaître, A., Boogard, T. (Eds) *Proceedings of the International Conference on*
836 *Landslide Processes: from geomorphologic mapping to dynamic modelling*, Strasbourg, CERG Editions, pp. 69-
837 74, 2009.

838 Niethammer, U., Rothmund, S., Schwaderer, U., Zeman, J., Joswig, M.: Open Source Image-Processing Tools
839 for Low-Cost UAV-Based Landslide Investigations. *International Archives of the Photogrammetry, Remote*
840 *Sensing and Spatial Information Sciences*, Volume XXXVIII-1/C22, 2011 ISPRS Zurich 2011 Workshop, 14-16
841 September 2011, Zurich, Switzerland, 161-166, 2011.

- 842 Nishar, A., Richards, S., Breen, D., Robertson, J. and Breen, B.: Thermal infrared imaging of geothermal
843 environments and by an unmanned aerial vehicle (UAV): A case study of the Wairakei - Tauhara geothermal
844 field, Taupo, New Zealand, *Renew. Energy*, 86, 1256–1264, doi:10.1016/j.renene.2015.09.042, 2016.
- 845 Nocerino, E., Menna, F., Remondino, F. and Saleri, R.: Accuracy and block deformation analysis in automatic
846 UAV and terrestrial photogrammetry - Lesson learnt. *ISPRS Annals of the Photogrammetry, Remote Sensing
847 and Spatial Information Sciences*, Vol. II(5/W1), Proc. 24th Intern. CIPA Symposium, 2–6 Sept., Strasbourg,
848 France. pp. 203-208. 2013
- 849 Obanawa, H., Y. Hayakawa, and C. Gomez.: 3D Modelling of inaccessible Areas using UAV-based Aerial
850 Photography and Structure from Motion. *Transactions of the Japanese Geomorphological Union*, 35, 283–
851 294. 2014.
- 852 Peters, M. P., Iverson, L. R., Matthews, S. N. and Prasad, A. M.: Wildfire hazard mapping: exploring site
853 conditions in eastern US wildland–urban interfaces, *International Journal of Wildland Fire*, 22, 567-578, 2013.
- 854 Pham, T.-T.-H., P. Apparicio, C. Gomez, C. Weber, and D. Mathon.: Towards a rapid automatic detection of
855 building damage using remote sensing for disaster management. The Haiti earthquake. *Dis. Prev. Manage*,
856 23, 53–66, 2014. doi: 10.1108/DPM-12-2012-0148
- 857 Piras, M., Taddia, G., Forno, M.G., Gattiglio, M., Aicardi, I., Dabove, P., Lo Russo, S. and Lingua, A.: Detailed
858 geological mapping in mountain areas using an unmanned aerial vehicle: application to the Rodoretto Valley,
859 NW Italian Alps, *Geomatics, Natural Hazards and Risk*, 8(1), 137-149, 2017.
- 860 Pollefeys, M., Gool, L. V., Vergauwen, M., Cornelis, K., Verbiest, F. and Tops, J.: Image-Based 3D Acquisition
861 of Archaeological Heritage and Applications. *Proc. Conf. on Virtual Reality, Archeology, and Cultural Heritage*,
862 255–262, 2001.
- 863 Pratt, K.S., Murphy, R., Stover, S. and Griffin, C.: Conops and autonomy recommendations for VTOL small
864 unmanned aerial system based on Hurricane Katrina operations, *Journal of Field Robotics*, 26(8), 636-650,
865 2009.
- 866 Pyo, J., Cho, H., Joe, H., Ura, T. and Yu, S.: Development of hovering type AUV “Cyclops” and its performance
867 evaluation using image mosaicing, *Ocean Eng.*, 109, 517–530, doi:10.1016/j.oceaneng.2015.09.023, 2015.
- 868 Rau, J.Y., Jhan, J.P., Lo, C.F. and Lin Y. S.: Landslide mapping using imagery acquired by a fixed-wing UAV,
869 *International Archives of the Photogrammetry, Remote Sensing and Spatial Information Sciences*, Volume
870 XXXVIII-1/C22, 2011 ISPRS Zurich 2011 Workshop, 14-16 September 2011, Zurich, Switzerland, 195-200,
871 2011.
- 872 Razak, K. A., Santangelo, M., Van Westen, C. J., Straatsma, M. W., and de Jong, S. M.: Generating an optimal
873 DTM from airborne laser scanning data for landslide mapping in a tropical forest environment,
874 *Geomorphology*, 190, 112-125, 25 <https://doi.org/10.1016/j.geomorph.2013.02.021>, 2013
- 875 Ryan, J. C., Hubbard, A. L., Box, J. E., Todd, J., Christoffersen, P., Carr, j. R., Holt, T. O., and Snooke, N.: Repeat
876 UAV photogrammetry to assess calving front dynamics at a large outlet glacier draining the Greenland Ice
877 Sheet, *The Cryosphere*, 9, 1-11, 2015.
- 878 Saiki, K. and Ohba, T.: Development of an unmanned observation aerial vehicle (UAV) as a tool for volcano
879 survey (in Japanese with English abstract), *Bull. Volcanol. Soc. Japan Second Ser.*, 55(3), 137–146, 2010.

880 Salvini, R., Mastrorocco, G., Seddaiu, M., Rossi, D. and Vanneschi, C.: The use of an unmanned aerial vehicle
881 for fracture mapping within a marble quarry (Carrara, Italy): photogrammetry and discrete fracture network
882 modelling, *Geomatics, Natural Hazards and Risk*, 8(1), 34-52, 2017.

883 Sanada, Y. and Torii T.: Aerial radiation monitoring around the Fukushima Dai-ichi nuclear power plant using
884 an unmanned helicopter, *Journal of Environmental Radioactivity*, 139, 294-299, 2015.

885 Santangelo, M., Cardinali, M., Rossi, M., Mondini, A. C., and Guzzetti, F.: Remote landslide mapping using a
886 laser rangefinder binocular and GPS, *Nat. Hazards Earth Syst. Sci.*, 10, 2539-2546, doi:10.5194/nhess-10-
887 2539-2010, 2010.

888 Saroglou, C., Asteriou, P., Zekkos, D., Tsiambaos, G., Clark, M., and Manousakis, J.: UAV-enabled
889 reconnaissance and trajectory modeling of a co-seismic rockfall in Lefkada, *Nat. Hazards Earth Syst. Sci.*
890 *Discuss.*, <https://doi.org/10.5194/nhess-2017-29>, in review, 2017.

891 Scaioni, M., Longoni, L., Melillo, V. and Papini, M.: Remote Sensing for Landslide Investigations: An Overview
892 of Recent Achievements and Perspectives, *Remote Sens.* 6(10), 9600-9652, 2014,

893 Schroeder, W., Oliva, P., Giglio, L., Quayle, B., Lorenz, E. and Morelli, F.: Active fire detection using Landsat-
894 8/OLI data, *Remote Sensing of Environment*, 185, 210-220, 2016.

895 Șerban, G., Rus, I., Vele, D., Brețcan, P., Alexe, M. and Petrea, D.: Flood-prone area delimitation using UAV
896 technology, in the areas hard-to-reach for classic aircrafts: case study in the north-east of Apuseni Mountains,
897 Transylvania, *Nat. Hazards*, 82(3), 1817–1832, doi:10.1007/s11069-016-2266-4, 2016.

898 Shinohara, H.: Composition of volcanic gases emitted during repeating Vulcanian eruption stage of
899 Shinmoedake, Kirishima volcano, Japan, *Earth Planets Sp.*, 65(6), 667–675, doi:10.5047/eps.2012.11.001,
900 2013.

901 Smith, M. W., Carrivick, J. L., Hooke, J. and Kirkby, M. J.: Reconstructing flash flood magnitudes using
902 “Structure-from-Motion”: A rapid assessment tool, *J. Hydrol.*, 519, 1914–1927,
903 doi:10.1016/j.jhydrol.2014.09.078, 2014.

904 Sohn, H., Heo, J., Yoo, H., Kim, S. and Cho, H.: Hierarchical multi-sensor approach for the assessment of flood
905 related damages, *Proc. XXI Congr.*, 207–210, 2008.

906 Stöcker, C., Bennett, R., Nex, F., Gerke, M. and Zevenbergen, J.: Review of the current state of UAV
907 regulations, *Remote Sensing* 9(5), 459, doi:10.3390/rs9050459, 2017.

908 Tang, L. and Shao, G.: Drone remote sensing for forestry research and practices. *J. For. Res.*, 26, 791-797,
909 2015.

910 Thamm, H.P. and Judex, M.: The “Low cost drone” – An interesting tool for process monitoring in a high
911 spatial and temporal resolution. *The International Archives of Photogrammetry, Remote Sensing and Spatial*
912 *Information Sciences*, Enschede, The Netherlands, Vol. XXXVI part 7. 2006

913 Tamminga, A. D., Eaton, B. C. and Hugenholtz, C. H.: UAS-based remote sensing of fluvial change following
914 an extreme flood event, *Earth Surf. Process. Landforms*, 40(11), 1464–1476, doi:10.1002/esp.3728, 2015.

915 Tannant, D. D., Giordan, D. and Morgenroth J.: Characterization and analysis of a translational rockslide on a
916 stepped-planar slip surface. *Engineering Geology*, 220, 144-151, 2017.

- 917 Tarolli, P.: High-resolution topography for understanding Earth surface processes: opportunities and
918 challenges, *Geomorphology*, 216, 295–312, 2014.
- 919 Tobita, M., Kamiya, I., Iwahashi, J., Nakano, T. and Takakuwa, N.: UAV aerial photogrammetry in Nishinoshima
920 Island and its analysis (in Japanese), *Bull. Geospatial Inf. Auth. Japan*, 125, 115–124, 2014a.
- 921 Tobita, M., Kamiya, I., Nakano, T., Iwahashi, J., Osumi, K. and Takakuwa, N.: Precise UAV aerial
922 photogrammetry in Nishinoshima Island (in Japanese), *Bull. Geospatial Inf. Auth. Japan*, 125, 145–154, 2014b.
- 923 Tokarczyk, P., Leitao, J. P., Rieckermann, J., Schindler, K. and Blumensaat, F.: High-quality observation of
924 surface imperviousness for urban runoff modelling using UAV imagery, *Hydrol. Earth Syst. Sci.*, 19(10), 4215–
925 4228, doi:10.5194/hess-19-4215-2015, 2015.
- 926 Torrero, L. Seoli, L. Molino, A. Giordan, D. Manconi, A. Allasia, P. and Baldo, M.: The Use of Micro-UAV to
927 Monitor Active Landslide Scenarios, in: *Engineering Geology for Society and Territory*, edited by: Lollino, G.,
928 Manconi, A., Guzzetti, F., Culshaw, M., Bobrowsky P., and Luino, F., Springer International Publishing
929 Switzerland, 5, 701-704, doi:10.1007/978-3-319-09048-1_136, 2015.
- 930 Török, Á., Barsi, Á., Bögöly, G., Lovas, T., Somogyi, Á., and Görög, P.: Slope stability and rock fall hazard
931 assessment of volcanic tuffs using RPAS and TLS with 2D FEM slope modelling, *Nat. Hazards Earth Syst. Sci.*
932 *Discuss.*, <https://doi.org/10.5194/nhess-2017-56>, in review, 2017.
- 933 Travelletti, J., Delacourt, C., Allemand, P., Malet, J.P., Schmittbuhl, J., Toussaint, R. and Bastard, M.:
934 Correlation of multi-temporal ground-based optical images for landslide monitoring: application, potential
935 and limitations, *ISPRS J Photogramm Remote Sens*, 70, 39-55, 2012.
- 936 Tu, J., Sui, H., Feng, W., Sun, K., Xu, C. and Han, Q.: Detecting building facade damage from oblique aerial
937 images using local symmetry feature and the Gini Index. *Remote Sensing Letters*, 8(7), 676-685, 2017.
- 938 Turner, D. and Lucieer, A.: Using a micro unmanned aerial vehicle (UAV) for ultra-high resolution mapping
939 and monitoring of landslide dynamics. In *Proceedings of the IEEE International Geoscience and Remote*
940 *Sensing Symposium*, Melbourne, Australia, 25 July 2013.
- 941 Turner, D., Lucieer, A. and Watson, C.: An automated technique for generating georectified mosaics from
942 ultrahigh resolution unmanned aerial vehicle (UAV) imagery, structure from motion (SfM) point
943 clouds. *Remote Sens.*, 4(12), 1392-1410, 2012.
- 944 Turner, D., Lucieer, A. and de Jong, S.M.: Time Series Analysis of Landslide Dynamics Using an Unmanned
945 Aerial Vehicle (UAV), *Remote Sensing*, 7(2), 1736-1757, 2015.
- 946 Van Den Eeckhaut, M., Poesen, J., Verstraeten, G., Vanacker, V., Nyssen, J., Moeyersons, J., van Beek, L. P. H.,
947 and Vandekerckhove, L.: Use of LIDAR-derived images for mapping old landslides under forest, *Earth Surf.*
948 *Proc. Land.*, 32, 754-769, <https://doi.org/10.1002/esp.1417>, 2007.
- 949 Van Westen J.C., Castellanos, E. and Kuriakose S.L.: Spatial data for landslide susceptibility, hazard, and
950 vulnerability assessment: An overview. *Engineering Geology*, 102(3–4), 112-131, 2008.
- 951 Vetrivel, A., Gerke, M., Kerle, N., Nex, F. and Vosselman, G.: Disaster damage detection through synergistic
952 use of deep learning and 3D point cloud features derived from very high resolution oblique aerial images,

953 and multiple-kernel-learning. *ISPRS Journal of Photogrammetry and Remote Sensing*, doi:
954 10.1016/j.isprsjprs.2017.03.001, in press.

955 Vetrivel, A., Gerke, M., Kerle, N. and Vosselman, G.: Identification of damage in buildings based on gaps in
956 3D point clouds from very high resolution oblique airborne images. *ISPRS Journal of Photogrammetry and*
957 *Remote Sensing*, 105, 61-78, 2015.

958 Walter, M., Niethammer, U., Rothmund, S. and Joswig, M.: Joint analysis of the Super-Sauze (French Alps)
959 mudslide by nanoseismic monitoring and UAV-based remote sensing. *EAGE First Break*, 27(8), 75-82, 2009.

960 Wen, Q., He, H., Wang, X., Wu, W., Wang, L., Xu, F., Wang, P., Tang, T. and Lei, Y.: UAV remote sensing hazard
961 assessment in Zhouqu debris flow disaster, in: *Remote Sensing of the Ocean, Sea Ice, Coastal Waters, and*
962 *Large Water Regions*, Bostater, C.R., Ertikas, S.P., Neyt X. and Velez-Reyes, M. (eds.), , 8 pp., 2011.

963 Westoby, M. J., Brasington, J., Glasser, N. F., Hambrey, M. J. and Reynolds, M. J.: Structure-from-Motion
964 photogrammetry: A low-cost, effective tool for geoscience applications. *Geomorphology*, 179, 300-314,
965 2012.

966 Wing, M. G., Burnett J. D. and Sessions, J.: Remote sensing and unmanned aerial system technology for
967 monitoring and quantifying forest fire impacts, *Int J Remote Sens Appl.*, 4(1), 18-35, 2014.

968 Witek, M., Jeziorska, J. and Niedzielski, T.: An experimental approach to verifying prognoses of floods using
969 an unmanned aerial vehicle, *Meteorol. Hydrol. Water Manag.*, 2(1), 3–11 [online] Available from:
970 [http://www.mhwm.pl/An-experimantal-approach-to-verifying-prognoses-of-floods-using-unmanned-aerial-](http://www.mhwm.pl/An-experimantal-approach-to-verifying-prognoses-of-floods-using-unmanned-aerial-vehicle,0,8.html)
971 [vehicle,0,8.html](http://www.mhwm.pl/An-experimantal-approach-to-verifying-prognoses-of-floods-using-unmanned-aerial-vehicle,0,8.html), 2014.

972 Woodget, A. S., Carbonneau, P. E., Visser, F. and Maddock, I. P.: Quantifying submerged fluvial topography
973 using hyperspatial resolution UAS imagery and structure from motion photogrammetry, *Earth Surf. Process.*
974 *Landforms*, 40, 47–64, doi:10.1002/esp.3613, 2015.

975 Yajima, R., Nagatani, K. and Yoshida, K.: Development and field testing of UAV-based sampling devices for
976 obtaining volcanic products, in 2014 IEEE International Symposium on Safety, Security, and Rescue Robotics,
977 27-30 Oct. 2014, Hokkaido, Japan, 1–5, 2014.

978 Xie, Z., J. Yang, C. Peng, Y. Wu, X. Jiang, R. Li, Y. Zheng, Y. Gao, S. Liu, and B. Tian.: Development of an UAS for
979 post-earthquake disaster surveying and its application in Ms7.0 Lushan Earthquake, Sichuan, China. *Comput.*
980 *Geosc.* 68, 22–30, 2014.

981 Yoon, W.S., Jeong, U.J. and Kim, J.H.: Kinematic analysis for sliding failure of multi-faced rock slopes,
982 *Engineering Geology*, 67, 51-61, 2002.

983 Zajkowski, T.J., Dickinson, M.B., Hiers, J.K., Holley, W., Williams, B.W., Paxton, A., Martinez, O. and Walker,
984 G.W.: Evaluation and use of remotely piloted aircraft systems for operations and research – RxCADRE 2012.
985 *International Journal of Wildland Fire*, 25, 114-128, 2015.

986 Zazo, S., Molina, J. L. and Rodríguez-González, P.: Analysis of flood modeling through innovative geomatic
987 methods, *J. Hydrol.*, 524, 522–537, doi:10.1016/j.jhydrol.2015.03.011, 2015.